

COMPACT SIZE ULTRA-WIDEBAND METAMATERIAL ANTENNA

by
Hakkı Toran

Submitted to the Institute of Graduate Studies in
Science and Engineering in partial fulfillment of
the requirements for the degree of
Master of Science
in
Electrical and Electronics Engineering

Yeditepe University
2012

COMPACT SIZE ULTRA-WIDEBAND METAMATERIAL ANTENNA

APPROVED BY:

Inst. Deniz Pazarıcı
(Advisor)



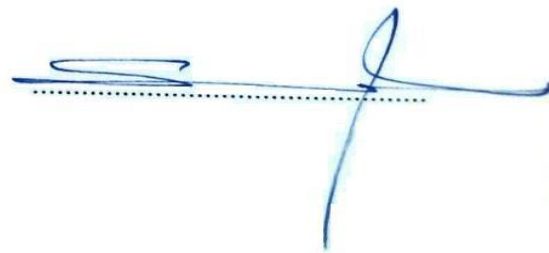
Asst. Prof. Dr. Serkan Topalođlu
(Co-Advisor)



Asst. Prof. Dr. Ali Akman



Assoc. Prof. Dr. Cahit Canbay



DATE OF APPROVAL: .../.../....

ACKNOWLEDGEMENTS

First and foremost, I would like to express my sincere thanks and gratitude to my advisor Inst. Deniz Pazarıcı for her guidance and encouragement

I would like to express sincere thanks and gratitude to my co-advisor Asst. Prof. Dr. Serkan Topaloğlu whom provided me opportunity to pursue my study and complete my thesis and guided me.

I would like to thank Asst. Prof. Dr. Ali Akman for his support, guidance and constructive advices.

I would like to give my special thanks to Assoc. Prof. Dr. Cahit Canbay for his constructive advices and suggestions.

I would like to thank Istanbul Technical University for providing measurement environment and equipment to test my antenna.

I would like to express my deepest gratitude to my parents for their support and encouragement whenever and wherever they are.

ABSTRACT

COMPACT SIZE ULTRA-WIDEBAND METAMATERIAL ANTENNA

In this thesis, fundamental concepts of metamaterials and electromagnetic wave propagation in metamaterial medium, brief theory of transmission lines, and CRLH transmission line approach to metamaterials are introduced. Using the concept of CRLH metamaterial, compact size ultra-wideband metamaterial antennas are designed and implemented. Antennas are excited by a coaxial feed. The shape of the antenna is tapered to provide impedance matching over a wider band. Furthermore ring slot is opened on the radiating part of the antenna; however spurious resonances emerged within the frequency band of the metamaterial antenna. Using rectangular split-ring slots instead of rectangular ring slots eliminated those unwanted resonances and improved the voltage standing wave ratio (VSWR) frequency bandwidth and gain of the antenna. The final antenna, compact size ultra-wideband antenna with split-ring slot, has VSWR value < 2 from 3.8GHz to 16.4GHz according to simulation results, 4GHz to 17.5GHz according to measurement results. Although the designed and realized antennas have very compact sizes overall dimensions of the antenna are just 18mm x 26.2mm, they can successfully cover a large spectrum. The final antenna has an omni-directional radiation pattern. During design a commercial 3D electromagnetic solver program FEKO was used to simulate the antenna and obtain antenna evaluate the results. Metamaterial antennas designed and simulated using FEKO, are fabricated on a FR4 substrate with dielectric constant $4.3\epsilon_0$ and thickness 1mm. Voltage standing wave ratio and input impedance of the fabricated antennas are measured using a network analyzer. The results obtained from measurement and simulation are in good agreement with each other.

ÖZET

KÜÇÜK BOYUTLU ÇOK GENİŞ BANTLI METAMALZEME ANTEN

Bu tezde metamalzemelerin temel prensipleri ve elektromanyetik dalgaların metamalzeme ortamındaki ilerleyişi, iletim hatlarının temelleri ve metamalzemelere kompozit iletim hatları methoduyla yaklaşım tanıtılmıştır. Bu tezde kompozit metamalzemeleri kullanarak koaksiyel hatla beslenen çok geniş bantlı anten tasarlanmıştır. Antenin daha geniş bantta empedans uyumluluğunu sağlayabilmek için antene konik bir şekil verilmiştir. Antenin daha geniş bir bantta empedans uyumunun olabilmesi ve kazanc sağlayabilmesi için anten üstünde dikdörtgen şeklinde yarık açıldı; antenin düşük frekanslardaki empedans uyumu iyileşti fakat diğer taraftan bu dikdörtgen şeklindeki yarık antenin frekans bandı içerisinde istenmeyen rezonanslar oluşturdu. Dikdörtgen şeklinde yarık yerine bölünmüş dikdörtgen şeklinde yarık kullanılması bu istenmeyen rezonanslar ortadan kaldırılmıştır ve antenin duran dalga frekans bandı ve kazancı iyileşmiştir. En sonunda ortaya çıkan anten küçük boyutlu ve çok geniş bantlı bölünmüş yarıklı bir antendir. Bölünmüş dikdörtgen şeklinde yarıklı küçük boyutlu çok geniş bantlı antenin benzetim sonuçlarına göre duran dalga oranı 3.8GHz'den 16.4GHz'e, ölçüm sonuçlarına göre ise 4GHz'den 17.5GHz'e kadar 2'nin altındadır. Bu anten çok yönlü ışına yapan bir antendir. Dizayn sürecinde anteni modellemek ve sonuçlarını değerlendirmek üzere ticari bir yazılım olan ve 3 boyutlu elektromanyetik problem çözücü FEKO yazılımı kullanılmıştır. FEKO programını kullanarak tasarlanan antenler 1mm kalınlığında dielektrik katsayısı $4.3\epsilon_0$ olan FR4 bir malzeme üzerine başılmıştır. Üretilmiş olan antenler vektor network analizörü kullanarak test edilmiş ve benzetim sonuçlarıyla oldukça tutarlı oldukları görülmüştür.

TABLE OF CONTENTS

ACKNOWLEDGEMENTS	iii
ABSTRACT.....	iv
ÖZET	v
TABLE OF CONTENTS.....	vi
LIST OF FIGURES	vii
LIST OF TABLES	xi
LIST OF SYMBOLS / ABBREVIATIONS	xii
1. INTRODUCTION	1
2. METAMATERIALS	3
2.1. METAMATERIAL DEFINITION	3
2.1.1. Electromagnetism in Left Handed Media	5
2.1.1.1. Refraction at a Metamaterial Interface	8
2.1.1.2. Doppler Effect in Metamaterial Medium	9
2.2. TRANSMISSION LINE METAMATERIALS.....	10
2.2.1. Transmission Line Theory	10
2.2.2. Right-Handed Transmission Lines	12
2.2.3. Left-Handed Transmission Lines.....	12
2.2.4. CRLH Transmission Lines	13
2.2.5. Permittivity and Permeability Calculation for LH Metamaterials.....	15
3. UWB ANTENNAS.....	17
3.1. INTRODUCTION TO UWB ANTENNAS	18
3.1.1. Frequency Independent Antennas.....	18
3.1.2. Multi-Resonant Antennas	19
3.1.3. Travelling Wave Antennas	19
3.1.4. Small Element Antennas.....	19
3.2. DEFINITION OF UWB ANTENNAS.....	19
4. UWB METAMATERIAL ANTENNA DESIGNS, SIMULATIONS	21
4.1. COMPACT SIZE UWB METAMATERIAL ANTENNA	21
4.1.1. VSWR Frequency Bandwidth.....	23

4.1.2. Gain.....	23
4.1.3. Determining the Contribution of LH metamaterial to the Antenna.....	24
4.1.3.1. VSWR Frequency Bandwidth.....	25
4.1.3.2. Gain.....	26
4.2. COMPACT SIZE UWB METAMATERIAL ANTENNA WITH RING SLOT.	27
4.2.1. VSWR Frequency Bandwidth.....	29
4.2.2. Gain.....	30
4.3. COMPACT SIZE UWB METAMATERIAL ANTENNA WITH SPLIT RING SLOT.....	31
4.3.1. VSWR Frequency Bandwidth.....	33
4.3.2. Gain.....	34
5. COMPACT SIZE UWB METAMATERIAL ANTENNA REALIZATION AND..... MEASUREMENTS.....	39
5.1. COMPACT SIZE UWB METAMATERIAL ANTENNA WITH RING SLOT.	39
5.2. COMPACT SIZE UWB METAMATERIAL ANTENNA WITH SPLIT RING SLOT.....	42
6. CONCLUSION.....	45
REFERENCES.....	50

LIST OF FIGURES

Figure 2.1.	Possible combinations of permittivity and permeability.....	5
Figure 2.2.	Comparison of wave propagation in right-handed and left-handed materials a. Conventional material, b. Metamaterial.....	8
Figure 2.3.	Comparison of wave refraction in conventional and left-handed material a. Conventional material, b. Metamaterial	9
Figure 2.4.	Equivalent circuit of a transmission line	10
Figure 2.5.	Equivalent circuit models of RH, LH and CRLH transmission lines a. RH transmission line, b. LH transmission line, c. CRLH transmission line.....	13
Figure 2.6.	Unit cell for a 2 dimensional distributed cell	15
Figure 4.1.	Compact Size UWB metamaterial antenna a. Top view, b. Bottom view	22
Figure 4.2.	Transparent view of compact size UWB metamaterial antenna	22
Figure 4.3.	Equivalent circuit model for compact size UWB metamaterial antenna.	23
Figure 4.4.	VSWR graphic of compact size UWB metamaterial antenna.....	23
Figure 4.5.	Total gain of compact size UWB metamaterial antenna.....	24
Figure 4.6.	View of the same antenna with metamaterial contribution removed a. Top view, b. Bottom view	25
Figure 4.7.	Transparent view of UWB metamaterial antenna with metamaterial	

contribution removed	25
Figure 4.8. Comparison of VSWR frequency bandwidth of the UWB metamaterial antenna and same antenna with metamaterial contribution removed.....	26
Figure 4.9. Comparison of total gain of the UWB metamaterial antenna and same antenna with metamaterial contribution removed.....	27
Figure 4.10. Compact size UWB Metamaterial antenna with ring slot a. Top view, b. Bottom view	28
Figure 4.11. Transparent view of compact size UWB metamaterial antenna with ring slot	28
Figure 4.12. Simulated VSWR of compact size UWB metamaterial antenna with ring slot	30
Figure 4.13. Total gain of compact size UWB metamaterial antenna with ring slot.....	31
Figure 4.14. Compact size UWB Metamaterial antenna with split-ring slot a.Top view, b.Bottom view	32
Figure 4.15. Transparent view of compact size UWB metamaterial antenna split-ring slot	33
Figure 4.16. VSWR of compact size UWB metamaterial antenna with split-ring slot	34
Figure 4.17. Total gain of compact size UWB metamaterial antenna with split-ring slot	35
Figure 4.18. Simulated radiation patterns at 4.2 GHz a. x-y plane, b. x-z plane, c. y-z plane, d. 3D radiation pattern	36

Figure 4.19. Simulated radiation patterns at 7.9 GHz a. x-y plane, b. x-z plane, c. y-z plane, d. 3D radiation pattern	37
Figure 4.20. Simulated radiation patterns at 12.2 GHz a. x-y plane, b. x-z plane, c. y-z plane, d. 3D radiation pattern	38
Figure 5.1. Compact size UWB metamaterial antenna with ring slots a. Top view, b. Bottom view	39
Figure 5.2 VSWR measurement result of compact size UWB metamaterial antenna with ring slot.....	40
Figure 5.3. Comparison of measured and simulated results for compact size UWB metamaterial antenna with ring slot	41
Figure 5.4. Compact size metamaterial antenna with split-ring slots.....	42
Figure 5.5 VSWR measurement result of compact size metamaterial antenna with split-ring slot.....	43
Figure 5.6. Measurement and simulated results comparison for compact size UWB split-ring-slotted antenna.....	44
Figure 6.1. Comparison of simulated VSWR results for all all designed antennas.....	46
Figure 6.2. Comparison of simulated gain for all designed antennas.....	47
Figure 6.3. Comparison of measured VSWR results for compact size UWB metamaterial antenna ring-slot and split-ring-slot.....	48

LIST OF TABLES

Table 4.1.	Dimension of metamaterial antenna with ring slots	29
Table 4.2.	Dimension of metamaterial antenna with split ring slots	32
Table 6.1.	Comparison of dimensions designed antennas.....	45
Table 6.2.	Summary of the performance for compact size UWB metamaterial antenna with split-ring slots	48

LIST OF SYMBOLS / ABBREVIATIONS

CAD	Computer-aided drawing
CPW	Coplanar waveguide
FCC	Federal Communications Commission
IEEE	Institute of electrical and electronics engineers
MOM	Moment of method
PCB	Printed circuit board
UWB	Ultra wideband
VSWR	Voltage standing wave ratio

1. INTRODUCTION

The amount of data transmitted and received through wireless communication systems is increasing very rapidly. Meanwhile wireless systems, especially the portable wireless devices, are getting more compact, low profile and low cost [1]. These increasing data traffic in wireless communication and shrinking size of wireless systems put forward new challenges in design of wireless system components. Especially, designing the radiating element antenna, which is capable of meeting requirements of this increasing high data traffic rates, in a limited space is getting more complex [2].

Microstrip antennas have been used widely in wireless communication systems [1,2], due to their low cost simple structure, compact size, low profile. However their compact sizes started to be unsatisfactory due to limited space on wireless systems [3-5]. That is why many techniques to reduce antenna size are offered. Printing antenna on a higher dielectric surface is one of the most conventional solutions to reduce antenna size; however this solution suffers from reduced bandwidth and efficiency. Furthermore characteristic impedance on a high dielectric medium is rather low which results difficulty in impedance matching of the antenna. Besides using high permittivity medium, another techniques are available to reduce antenna size, however they increase design complexity.

Impedance bandwidth of the printed antennas needs to be enhanced in order to be used successfully in UWB antennas design. Printed planar monopole antennas are may be a candidate to be applied for UWB antenna designs however they may suffer from size [5,6].

Metamaterials are man-made artificial structures and they are not found in nature. In nature the permittivity and the permeability of most materials are positive. The material with positive permittivity and permeability are referred as right-handed material (RH). It is also possible to encounter that metamaterials are sometimes called left-handed (LH) materials [7,8]. Because metamaterials reflect waves in a way counter to conventional materials which obey the right hand rule of the electromagnetism. Metamaterials exhibiting LH and RH behavior simultaneously are called as composite right left-handed (CRLH) metamaterials [7,8].

Metamaterials started to be used in electromagnetic especially in antenna designs due their unusual electromagnetic properties [7,9]. Different from the conventional materials, metamaterials refract electromagnetic waves counter to the conventional materials and have negative phase velocity [9,10]. Also metamaterials makes it possible to design compact size antennas for example using zeroth order resonance mode (ZOR) which allows to design size independent antennas [11]. Thus the size of the antennas can be miniaturized [12,13]. In literature there many works in which metamaterials antennas improves antennas efficiency and gain [14,15]. In addition to gain and efficiency, return loss of the resonant type antenna can be improved by the incorporation of metamaterials [16]. Those unusual properties and benefits of the metamaterials started to be successfully tailored and used to improve the performance of the antennas in terms of impedance bandwidth, gain, and allow to design more compact antennas [17,18].

Using metamaterials in UWB antenna designs improves the antennas performance, in terms of bandwidth gain and reduces size of the antenna [19-21]. Moreover split-ring slots and tapered shapes can be employed in the antenna design to enhance the frequency bandwidth of the antenna [22].

CRLH metamaterials are a very good candidate to design compact size antennas [8,21]. However these metamaterial antennas may suffer from narrow bandwidth [21]. In this thesis, in order to increase the bandwidth, antenna has a tapered shape and split ring slot is etched on a tapered radiating part. Furthermore, it was many times proved and showed that CRLH metamaterial improves the antennas return loss and gain [14].

In literature, several types and designs of printed UWB antennas discussed [2-3,8,22-24]. For example; bi-conical antennas received considerable attention due to their well matching impedance bandwidths [24]; however bi-conical antennas are not applicable to use for portable wireless devices due to sizes and most of them are dimensional structures [25-27]. Furthermore log periodic antennas or antennas designed using log periodical antenna intuition can be used to design UWB antennas successfully however their size are large and not applicable to use in compact size application [24,28-29]. In order to reduce the size of the antennas CRLH metamaterial is used [17], but their size reduction level is inadequate compared with the antenna proposed in this thesis. Electromagnetic band gap

metamaterial (EBG) structures may also be used design UWB antennas [30], however these types of antennas are difficult to implement and for some applications they may suffer from their size like wireless USB application. Also another antenna design for wireless USB have dimension bigger than the antenna proposed in this thesis moreover its VSWR frequency bandwidth is much smaller than the antenna presented here [31].

2. METAMATERIALS

2.1. METAMATERIAL DEFINITION

Metamaterials are man-made artificial structures and they are not found in nature [17, 32, 33]. They are artificially manufactured. The Greek word “Meta” means beyond. Metamaterial means beyond the material.

Electrical and magnetic properties of materials are determined by permeability and permittivity value of the materials as shown in Figure 2.1. Permittivity and permeability may also be called as electric permittivity and magnetic permeability respectively. In nature the permittivity and the permeability of most materials are positive. The material with positive permittivity and permeability are referred as right-handed material (RHM). It is also possible to encounter that metamaterials are sometimes called left-handed materials. Because metamaterials reflect waves in a way counter to conventional materials which obey the right hand rule of the electromagnetism [42].

Permeability is a measure of material response to an applied magnetic field to support formation of magnetic field within itself,

$$\vec{B} = \mu \vec{H} \quad (2.1)$$

where as \vec{B} , is magnetic field, $\mu = \mu_0 \mu_r$, μ_0 is $4\pi \cdot 10^{-7}$ (H/m) permeability of the free space, μ_r is relative permeability, \vec{H} is magnetic field (B/m) [34].

Permittivity: is measure of resistance of material to form an electric field inside when an external electric field is applied

$$\vec{D} = \epsilon \vec{E} \quad (2.2)$$

Where as \vec{D} is electric displacement (C / m²), $\epsilon = \epsilon_0 \epsilon_r$, ϵ_0 is permittivity of the free space

and its value is $8,85 \cdot 10^{-12}$ (F/m) and ϵ_r is relative permittivity, and \vec{E} is electric field (V/m). Permittivity and permeability determine how a material will interact with electromagnetic radiation. According to permittivity and permeability values materials can be classified into four groups as shown in Figure 2.1. [21,34].

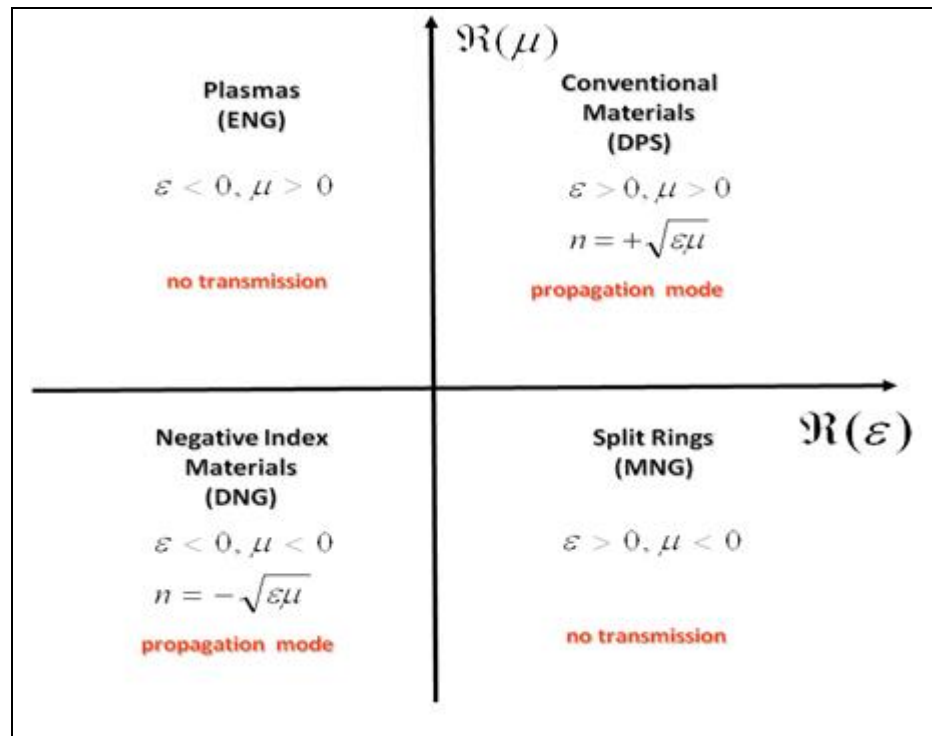


Figure 2.1. Possible combinations of permittivity and permeability

Most of the existing materials are in the first quadrant. Metamaterials are in the third quadrant of the graphic shown above in Figure 2.1.

2.1.1. Electromagnetism in Left-Handed Media

The propagation constant, k , of a plane wave is given by $k = \omega\sqrt{\epsilon\mu}$, where ϵ and μ are electrical permeability and magnetic permittivity of the material. Refractive index of the material is defined as $n = \pm\sqrt{\epsilon\mu}$. Also refractive index of a medium is defined as the ratio of the speed of light to the phase velocity [34, 35]. Maxwell equations for source free region in differential form are given below.

$$\nabla \times \vec{E} = -\frac{\partial \vec{B}}{\partial t} \quad (2.3)$$

$$\nabla \times \vec{H} = \frac{\partial \vec{D}}{\partial t} \quad (2.4)$$

$$\nabla \cdot \vec{D} = 0 \quad (2.5)$$

$$\nabla \cdot \vec{B} = 0 \quad (2.6)$$

Helmholtz equations can be obtained from the above Maxwell equations and given in frequency domain as in equation (2.7) and (2.8).

$$\nabla^2 \vec{E} + w^2 \mu \epsilon \vec{E} = 0 \quad (2.7)$$

$$\nabla^2 \vec{H} + w^2 \mu \epsilon \vec{H} = 0 \quad (2.8)$$

Solutions of the Helmholtz equations show how electric and magnetic fields propagate in a homogeneous material.

$$\nabla^2 \vec{E} + k^2 \vec{E} = 0 \quad (2.9)$$

$$\nabla^2 \vec{H} + k^2 \vec{H} = 0 \quad (2.10)$$

Where as $k^2 = w^2 \mu \epsilon$. Then wave number can be given as $k = \mp w \sqrt{\mu \epsilon}$. For metamaterials case negative valued one $k = -w \sqrt{\mu \epsilon}$ is the solution.

In general, plane wave fields are described as in equation (2.11) and (2.12) [3].

$$\vec{E} = \vec{E}_o e^{(-j\vec{k} \cdot \vec{r} + j\omega t)} \quad (2.11)$$

$$\vec{H} = \vec{H}_o e^{(-j\vec{k} \cdot \vec{r} + j\omega t)} \quad (2.12)$$

The curl of the equations (2.1) and (2.2) yields the equations below.

$$\vec{\nabla} \times \vec{H} = j\omega \epsilon \vec{E} \quad (2.13)$$

$$\vec{\nabla} \times \vec{E} = -j\omega \mu \vec{H} \quad (2.14)$$

The following equations (2.15) and (2.16) can be obtained from the above equations. It is seen from the equations below, those equations (2.13) and (2.14) for positive values of ϵ and μ ; \vec{E} , \vec{H} and \vec{k} form a right-handed orthogonal vectors as shown in Figure 2.2a..

$$\vec{k} \times \vec{H} = -\omega \epsilon \vec{E} \quad (2.15)$$

$$\vec{k} \times \vec{E} = \omega \mu \vec{H} \quad (2.16)$$

For negative values of ϵ and μ the equations (2.15) and (2.16) will be slightly modified to following equations (2.17) and (2.18). As a result \vec{E} , \vec{H} and \vec{k} form a left-handed orthogonal vectors as shown in Figure 2.2b.

$$\vec{k} \times \vec{H} = \omega |\epsilon| \vec{E} \quad (2.17)$$

$$\vec{k} \times \vec{E} = -\omega |\mu| \vec{H} \quad (2.18)$$

Direction of energy and power flow of an electromagnetic wave is determined by poynting vector [3, 5].

Poynting vector is given by the Equation (2.19). Thus direction of the poynting vector is independent of the values of ϵ and μ . In conventional material direction of wave propagation is same with the direction of the power flow, however in metamaterials direction of the wave propagation is opposite with the power flow.

$$\vec{S} = \vec{E} \times \vec{H} \quad (2.19)$$

In Figure 2.2. direction of the wave propagation and the poynting vectors are shown and compared for conventional materials and metamaterials [34,36,43].

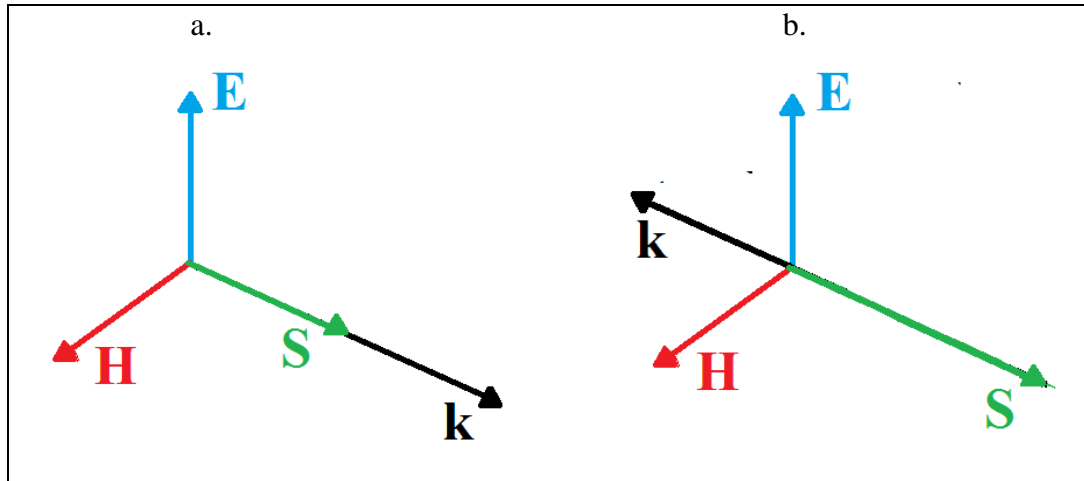


Figure 2.2. Comparison of wave propagation in right-handed and left-handed materials a. Conventional material, b. Metamaterial

2.1.1.1. Refraction at a metamaterial interface

Refractive index of material $n = \pm\sqrt{\epsilon\mu}$, determines how waves will travel from one medium to another. Naturally available materials possess positive permittivity and permeability thus they have positive refractive index. However metamaterials have negative permittivity and permeability which results a negative refractive index. Veselago showed that that negative refractive index is possible if a medium has both negative permittivity and permeability. Snell's Law given in equation (2.20) describes how an electromagnetic wave will behave when traversing the interface from a material with refractive index n_1 to another material refractive index n_2 [18, 36].

$$n_1 \sin\theta_1 = n_2 \sin\theta_2 \quad (2.20)$$

As shown in Figure 2.3. metamaterials reflect wave in the reverse direction when compared with conventional materials.

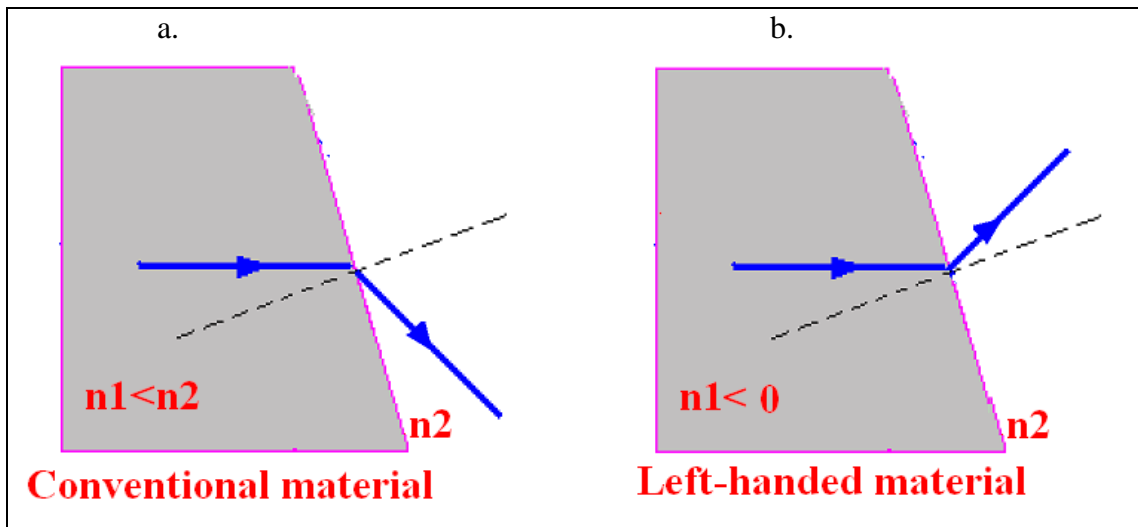


Figure 2.3. Comparison of wave refraction in conventional and left-handed materials
a. Conventional material, b. Metamaterial

2.1.1.2. Doppler effect in metamaterial medium

In a uniform medium, change in the frequency of a wave for an observer relative to the source of wave is defined as Doppler effect or Doppler shift. The frequency shift experienced by the observer depends on the relative velocity of the observer with respect to source of wave. Frequency shift can be calculated using the formula given in Equation (2.21),

$$\Delta\omega = \omega_0 \frac{nv}{c} \quad (2.21)$$

where ω_0 frequency of the radiation from source, v is velocity of the receiver towards to source, c is the speed of light in free space, n is the refractive index of the medium, $\Delta\omega$ is the difference between the source frequency and the frequency detected by the observer.

In metamaterials value of refractive index n is negative, thus from equation (2.21) it is apparently seen that frequency shift will be negative for positive values of observers' velocity v . As a result, in metamaterial medium Doppler shift is reversed [5].

2.2. TRANSMISSION LINE METAMATERIALS

Conventional transmission lines are known as right-handed transmission lines since they obey the right hand rule of electromagnetism. Transmission line is a material medium or structure which forms a path from one place to another for directing the transmission of energy, such as electromagnetic waves or mechanical waves [7].

2.2.1. Transmission Line Theory

At low frequency applications; the signal voltage on wire is same at every points of the wire, however at high frequency applications, the signal voltage may not be same at every single point on the wire. This depends on the comparison between the size of the wire and frequency. A general rule is, if the length of the wire is larger than the 1/10 of the applied wavelength, the wire should be treated as a transmission line [22].

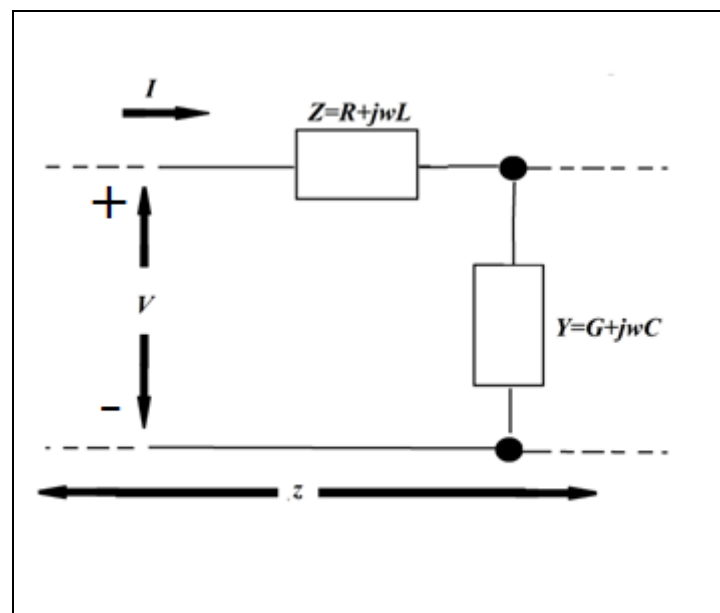


Figure 2.4. Equivalent circuit of a transmission line

Z and Y are the impedance for per unit length and defined in equations (2.22) and (2.23).

$$Z = R + j\omega L \quad (2.22)$$

$$Y = G + j\omega C \quad (2.23)$$

where as R is series resistance per unit length, L is series inductance per unit length, G is conductance per unit length ; C is shunt capacitance per unit length.

$$\frac{dV}{dz} = ZI \quad (2.24)$$

$$\frac{dI}{dz} = YV \quad (2.25)$$

Combining equations (2.24) and (2.25). Equations (2.26) and (2.27) are obtained.

$$\frac{d^2V}{dz^2} = ZYV \quad (2.26)$$

$$\frac{d^2I}{dz^2} = ZYI \quad (2.27)$$

Solution for equation (2.25) and (2.26) is given in equations (2.28) and (2.29).

$$V(z) = V_+ e^{\omega t - j\gamma z} + V_- e^{\omega t + j\gamma z} \quad (2.28)$$

$$I(z) = I_+ e^{\omega t - j\gamma z} + I_- e^{\omega t + j\gamma z} \quad (2.29)$$

$$\gamma = \alpha + j\beta = \sqrt{ZY} \quad (2.30)$$

Whereas γ is the propagation constant given with the equation (2.29) for lossless medium, and β is phase constant.

2.2.2. Right-Handed Transmission Lines

Conventional materials have positive values of ϵ and μ , as a result refractive index, $n = \pm\sqrt{\epsilon\mu}$, for these materials is a positive value. In conventional materials propagation

of electromagnetic waves obeys the right handed rule of electromagnetic and creates a right-handed orthogonal system of vectors for $(\vec{E}, \vec{H}, \vec{k})$ vector fields. Such materials are also called right-handed. In right-handed materials the propagation of the wave and energy is in the same direction as shown in Figure 2.2. As a result materials with positive values of ϵ and μ are right-handed materials.

2.2.3. Left-Handed Transmission Lines

In 1968 a Russian scientist Victor Veselago proposed the concept of metamaterials, their potential use in electromagnetic due to their unusual electromagnetic properties. Veselago proposed that metamaterials can be synthesized by using conventional material which they have positive values of permittivity and permeability [19]. Metamaterial based transmission lines attracted attention, because they are easy to fabricate, low cost.

In contrast to right-handed materials, metamaterials can exhibit a negative refractive index with permittivity ϵ and permeability μ being simultaneously negative. Their phase velocity direction is opposite to the direction of the signal energy propagation where the relative directions of the $(\vec{E}, \vec{H}, \beta)$ vector fields follow the left handed rule. Thus, metamaterials are also called “left-handed” (LH) materials [8].

The transmission line approach to implement LHM was first proposed at University of Toronto in 2002. In the proposed method, field components like E and H are mapped to the voltages and currents of the equivalent distributed L-C network.

2.2.4. CRLH Transmission Lines

Actually, purely left-handed transmission lines are not available and realizable physically. Because every left-handed metamaterial transmission line have right-handed properties due to the inevitable parasitic effects. Material which have right handed and left handed properties at the same time are called composite right left hander, CRLH, material. Left-handed metamaterials may be considered as simplified models of the CRLH materials [7]. CRLH transmission lines are realistic transmission lines.

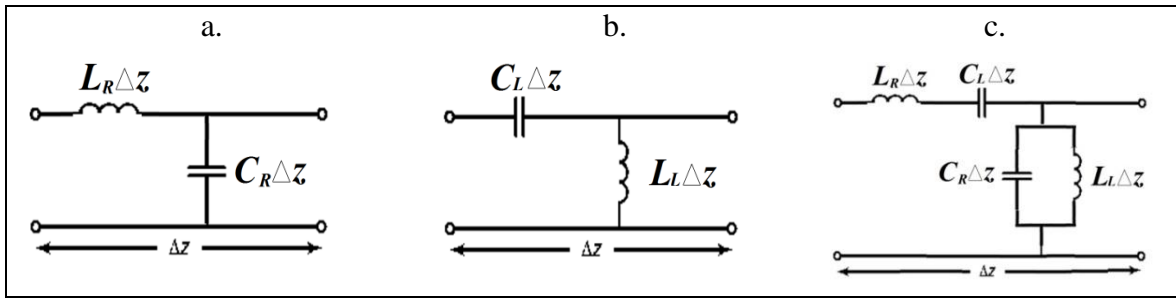


Figure 2.5. Equivalent circuit models of RH, LH and CRLH transmission lines a. RH transmission line, b. LH transmission line, c. CRLH transmission line

In order to better understand the CRLH transmission lines, transmission lines are compared using infinitely small circuit model.

In Figure 2.4. the equivalent circuit models for RH, LH, and CRLH lossless transmission lines are showed which are developed using conventional infinitesimal circuit model.

Assuming $Z(\omega)$ and $Y(\omega)$ represent the series impedance and shunt admittance for CRLH transmission line illustrated in Figure 2.4., the following equations can be concluded [7].

$$Z(\omega) = j \left(\omega L_R - \frac{1}{\omega C_L} \right) \quad (2.31)$$

$$Y(\omega) = j \left(\omega C_R - \frac{1}{\omega L_L} \right) \quad (2.32)$$

Series and shunt resonance frequencies for the CRLH transmission line in Figure 2.4. can be given with following equations (2.33) and (2.34).

$$\omega_{se} = \frac{1}{\sqrt{L_R C_L}} \quad (2.33)$$

$$\omega_{sh} = \frac{1}{\sqrt{L_L C_R}} \quad (2.34)$$

Some variables can be introduced as in equations (2.35) and (2.36) to simplify the solution.

$$\omega_L = \frac{1}{\sqrt{L_L C_L}} \quad (2.35)$$

$$\omega_R = \frac{1}{\sqrt{L_R C_R}} \quad (2.38)$$

The propagation constant γ was given to be equal to $\gamma = \alpha + j\beta = \sqrt{ZY}$, in equation (2.30). It can be expressed in terms of per length impedances and admittances as in presented in equation (2.36),

$$\gamma = \alpha + j\beta(\omega) = \sqrt{ZY} = js(\omega) \sqrt{\left(\frac{\omega}{\omega_R}\right)^2 + \left(\frac{\omega_L}{\omega}\right)^2 - \left(\frac{C_R}{C_L} + \frac{L_R}{L_L}\right)} \quad (2.36)$$

where α is attenuation constant and zero for lossless medium.

$$\beta(\omega) = s(\omega) \sqrt{\left(\frac{\omega}{\omega_R}\right)^2 + \left(\frac{\omega_L}{\omega}\right)^2 - \left(\frac{C_R}{C_L} + \frac{L_R}{L_L}\right)} \quad (2.37)$$

$$s(\omega) = \begin{cases} -1 & \text{if } \omega < \min(\omega_{se}, \omega_{sh}) & \text{LH range} \\ 0 & \text{if } \min(\omega_{se}, \omega_{sh}) < \omega < \max(\omega_{se}, \omega_{sh}) \\ +1 & \text{if } \omega > \max(\omega_{se}, \omega_{sh}) & \text{RH range} \end{cases} \quad (2.38)$$

The response how material as a function of frequency is given in equation (2.38). It can be seen from the equation (2.38) that a CRLH metamaterial may behave like a left-handed and right-handed material.

2.2.4. Permittivity and Permeability Calculation for LH Metamaterials

Dielectric material properties like permittivity and permeability can be modeled by LC networks [19,36,37]. Free space can be represented by L-C distributed networks. In this

case characteristic impedance of the network is equal to free space wave impedance. [19,36,37]. For LH materials permittivity and permeability of the materials can be determined using the analogy between the behavior of the wave on a LH transmission line and solution of a plane wave [38].

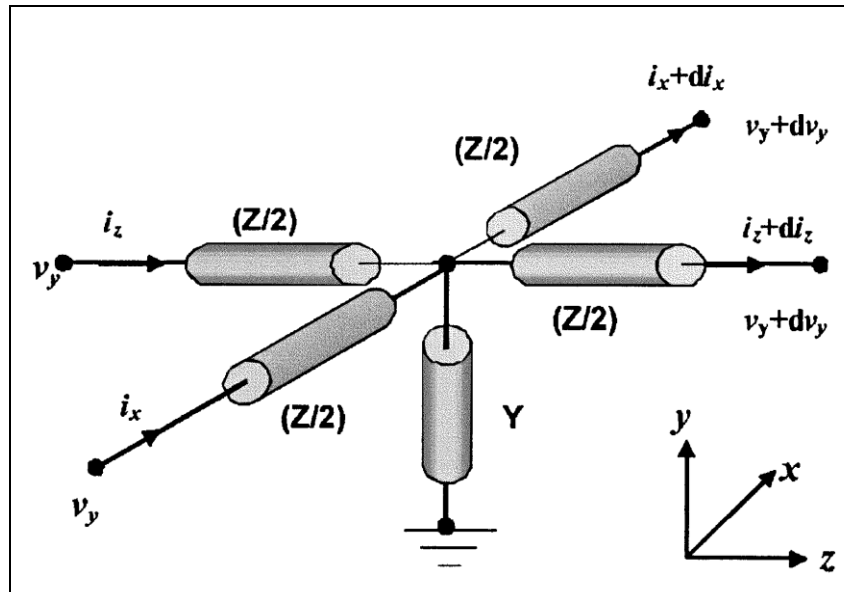


Figure 2.6. Unit cell for a 2 dimensional distributed cell [38]

Current and voltage relationships according to Figure 2.6. is given in the following equations.

$$\frac{\partial v_y}{\partial z} = -i_z Z \quad (2.39)$$

$$\frac{\partial v_y}{\partial x} = -i_x Z \quad (2.40)$$

$$\frac{\partial i_z}{\partial z} + \frac{\partial i_x}{\partial x} = -v_y Y \quad (2.41)$$

Combining the above equations the following equations are obtained

$$\frac{\partial^2 v_y}{\partial x^2} + \frac{\partial^2 v_y}{\partial x^2} + \beta^2 v_y = 0 \quad (2.42)$$

$$\beta = \pm \sqrt{-ZY} \quad (2.43)$$

Where β is the propagation constant. Field components can be mapped to the voltages and the currents in the medium. In a thin homogeneous isotropic medium, solution for a quasi-static transverse magnetic TM_y field maps v_y to E_y by using the definition of potential difference, and i_x to H_z and i_z to $-H_x$ by using the definition of Ampere's Law. As a result equations (2.39), (2.40), and (2.41) can be represented as in equations (2.44), Equation (2.45) and Equation (2.46) after mapping.

$$\frac{\partial E_y}{\partial x} = -j\omega\mu_s H_z \quad (2.44)$$

$$\frac{\partial E_y}{\partial z} = j\omega\mu_s H_x \quad (2.45)$$

$$\frac{\partial H_x}{\partial z} - \frac{\partial H_z}{\partial x} = j\omega\epsilon_s E_y \quad (2.46)$$

From the equations above, effective parameters of the material can be derived as below in Equation (2.47) and Equation (2.47).

$$j\omega\mu_s = Z \quad (2.47)$$

$$j\omega\epsilon_s = Y \quad (2.48)$$

The impedance and admittance of the equivalent circuit for left-handed materials given in Figure 2.5b., can be expressed as in equation (2.49) and equations (2.50).

$$Z = \frac{1}{j\omega C} \quad (2.49)$$

$$Y = \frac{1}{j\omega L} \quad (2.50)$$

Russian scientist Veselago postulated negative permittivity and permeability for metamaterials. Results in Equation (2.50) and Equation (2.51) for permittivity and permeability agree with the outcomes of the Veselago. Permeability in Equation (2.51) derived from the Equation (2.47) and Equation (2.49) shows that for left-handed materials have negative values permeability. Furthermore from Equation (2.48) and Equation (2.50), it is proved that left-handed materials have negative values of permittivity [26].

$$\mu_s = -\frac{1}{\omega^2 C} \quad (2.51)$$

$$\epsilon_s = -\frac{1}{\omega^2 L} \quad (2.52)$$

In nature purely left-handed materials are difficult to obtain due to parasitic capacitances and inductances. Every left-handed material has right-handed property due to parasitic effects. CRLH materials have negative values of permittivity and permeability for a certain frequency region [39]. The range of frequency where CRLH metamaterial can behave like LH material or RH material is given in equation (2.38).

3. UWB ANTENNAS

3.1. INTRODUCTION TO UWB ANTENNAS

An antenna is a transmitter used for radiating and receiving electromagnetic waves. Increasing commercial UWB applications has increased demand for ultra-wideband antennas [40]

First UWB radio developed by Guglielmo Marconi was a pulse-based radio in late 1800's. Although this Spark Gap radio was used several decades to transmit Morse codes, Spark Gap radio was forbidden in many applications due to interference to narrowband and its strong emission [40, 41].

In 1960s study of time domain electromagnetics initiated the modern UWB techniques and ongoing years this techniques were developed. Antenna designers like Rumsey and Dyson used these techniques in their research about logarithmic spiral antenna design and made their contribution to design wideband radiating antenna elements [40,41].

According to radiation characteristic UWB antennas can be categorized as; frequency independent antennas, multi resonant antennas, travelling wave antennas and small element antennas.

3.1.1. Frequency Independent Antennas

Bi-conical, spiral, conical, log periodic antennas are examples of frequency independent antennas and they are classical broadband and UWB antennas. Frequency independent antennas can operate over an extremely large frequency range, however they have some limitations. Frequency independent antennas are large antennas relative to their wavelength. Furthermore frequency independent antennas radiate different frequency components from different parts of the antenna, that is high frequency components are radiated from small parts of the antenna and low frequency components are radiated from large-scaled parts of

the antenna. Thus frequency independent antennas tends to be dispersive and can be used for dispersion tolerant applications.

3.1.2. Multi-Resonant Antennas

Multi resonant antennas consist of multiple narrowband radiating elements. Phase center of multi-resonant antennas are not fixed thus this type of antennas have dispersive characteristics.

3.1.3. Travelling-Wave Antennas

Travelling wave antennas are directional antennas and can be used for UWB applications. Examples of UWB antennas are horn antennas, tapered slot antennas. This type of antennas have very low dispersion and phase center variation.

3.1.4. Small Element Antennas

Small element antennas are evolution of monopole and basic dipole antenna. Examples of small element antennas are biconical and bow-tie antennas, Mather's diamond dipole, Stohr's spherical and ellipsoidal antennas, and Thomas's circular dipole. []

3.2. DEFINITION OF UWB ANTENNAS

Desired operating frequencies which are commonly used for UWB applications and UWB antennas are given below [43].

- U.S. FCC regulation 3.1 GHz to 10.6 GHz
- European regulation 6 GHz to 8.5 GHz
- Special allocations: for some radar applications..e.g

However the operating frequency of an UWB antenna is not limited to the above. The most general definition for UWB antenna is given as an antenna which has at least

500MHz frequency bandwidth and fractional bandwidth greater than 0.2. This is summarized in Equations (3.1), and Equation (3.1).

$$(f_H - f_L) \geq 500 \text{ MHz} \quad (3.1)$$

$$BW = 2 \frac{(f_H - f_L)}{(f_H + f_L)} \geq 0.25 \quad (3.1)$$

where as f_H and f_L are upper and lower operating band limits of the antenna.

4. COMPACT SIZE UWB METAMATERIAL ANTENNA DESIGNS, SIMULATIONS

An UWB microstrip patch antenna using CRLH transmission line metamaterial concepts is designed and antennas are fabricated on a conventional FR4 substrate. Patch antennas can be analyzed analytically using method of moments and cavity methods; however designing an antenna using these methods is difficult and time consuming. That is why during the design phase a 3D electromagnetic solver program called FEKO is used to determine the most suitable dimensions and radiation pattern, input impedance, VSWR parameters of the antenna.

4.1. COMPACT SIZE UWB METAMATERIAL ANTENNA

The antenna shown in the Figure 4.1. and Figure 4.2. has a metallic cell in the middle of the antenna. There is a gap between the metallic cell and the antenna. The gap between the metallic cell and the surrounding metallic structure creates a capacity which is a critical parameter for the matching of the antenna. Furthermore the capacitance created by this gap makes a contribution for left-handed material property. This metallic cell is connected with a via to the bottom of the antenna in order to provide ground potential to the metallic cell in the middle of the antenna. This antenna structure can be modeled using equivalent circuit model of CRLH metamaterial structures, because the gap between the cell and the surrounding metal acts as the left-handed series capacitor, and the via plays the role of a shunt inductance. The equivalent circuit of the antenna shown in Figure 4.1. and Figure 4.2. is given in Figure 4.3.. Both these series capacitor and the shunt inductance correspond to LH contribution, and the series inductance and the distributed shunt capacitance of the antenna results RH contribution. Antenna is excited by a pin feed as seen from Figure 4.2..

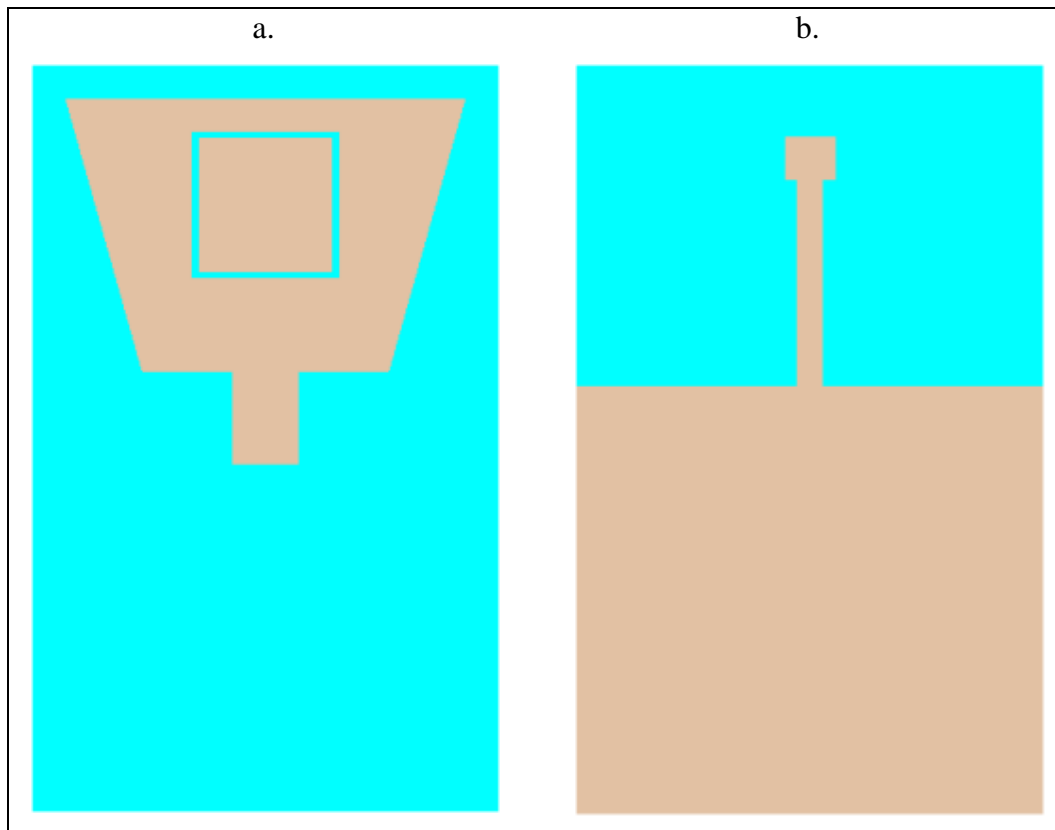


Figure 4.1. Compact size UWB metamaterial antenna a. Top view, b. Bottom view

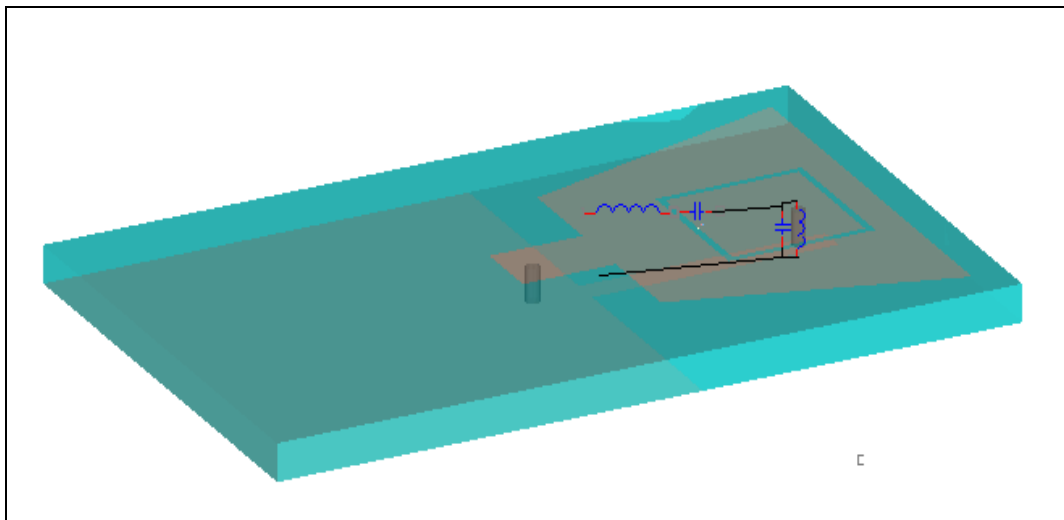


Figure 4.2. Transparent view of the compact size UWB metamaterial antenna

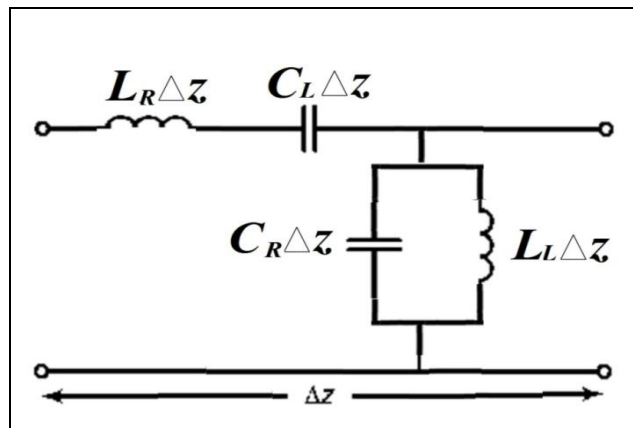


Figure 4.3. Equivalent circuit model for compact size UWB metamaterial antenna

4.1.1. VSWR Frequency Bandwidth

The VSWR frequency bandwidth of the compact size UWB metamaterial antenna is given in the Figure 4.4. VSWR value of the antenna is lower than 2 from 4 GHz to 11.5GHz. Frequency bandwidth of the antenna is 7.5GHz.

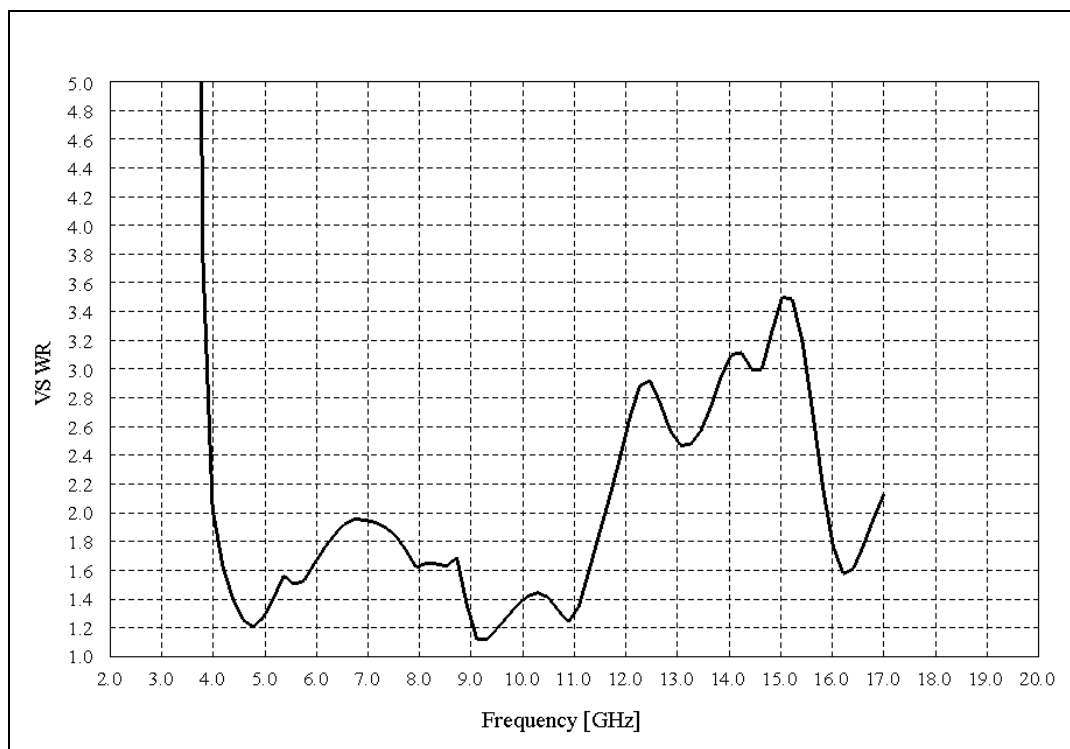


Figure 4.4. VSWR graphic of compact size UWB metamaterial antenna

4.1.2. Gain

In general gain of antenna can be expressed as ratio of the power produced by the antenna to the power produced by hypothetical lossless isotropic antenna. Total gain of the antenna is given in Figure 4.5. the antenna has a gain greater than 0 dBi in all its VSWR frequency bandwidth. The antenna has gain up to 13.8GHz.

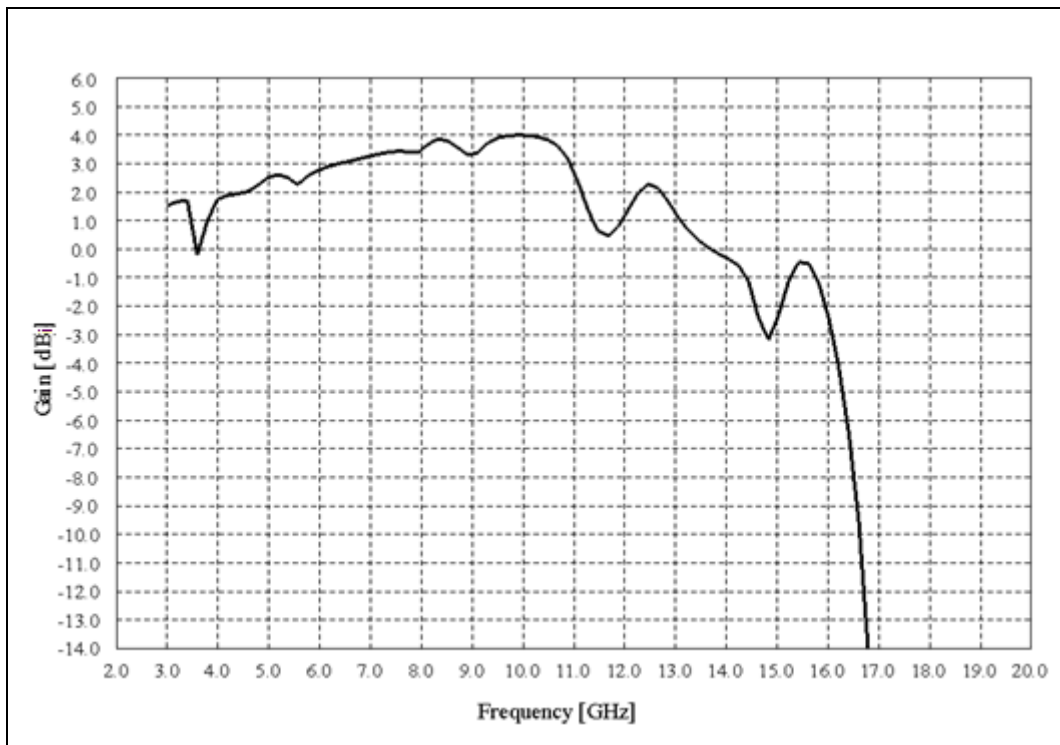


Figure 4.5. Total gain of the compact size UWB metamaterial antenna

4.1.3. Determining the contribution of LH metamaterial to the antenna

In order to determine the metamaterial effect in the design of the antenna, metallic cell on the upper side of the antenna is unified with the surrounding metal and the via between the metallic cell and the ground potential is removed. In other words, metamaterial properties removed from the antenna. The resulting designed antenna is shown in Figures 4.6. and Figures 4.7.

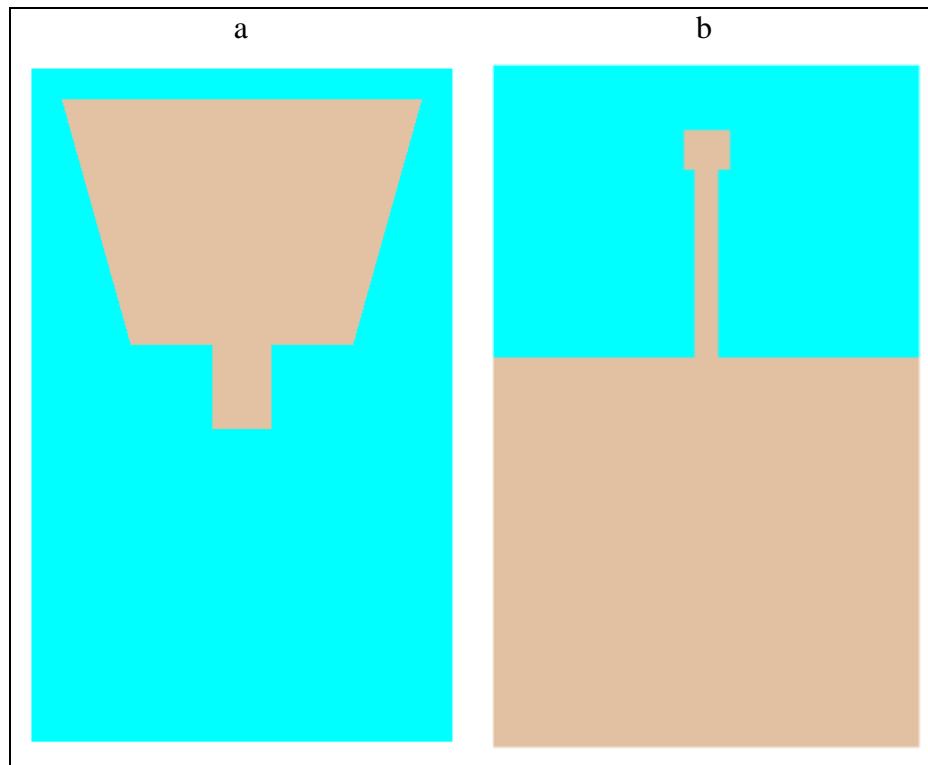


Figure 4.6. View of the same antenna with metamaterial contribution removed a. Top view, b. Bottom view

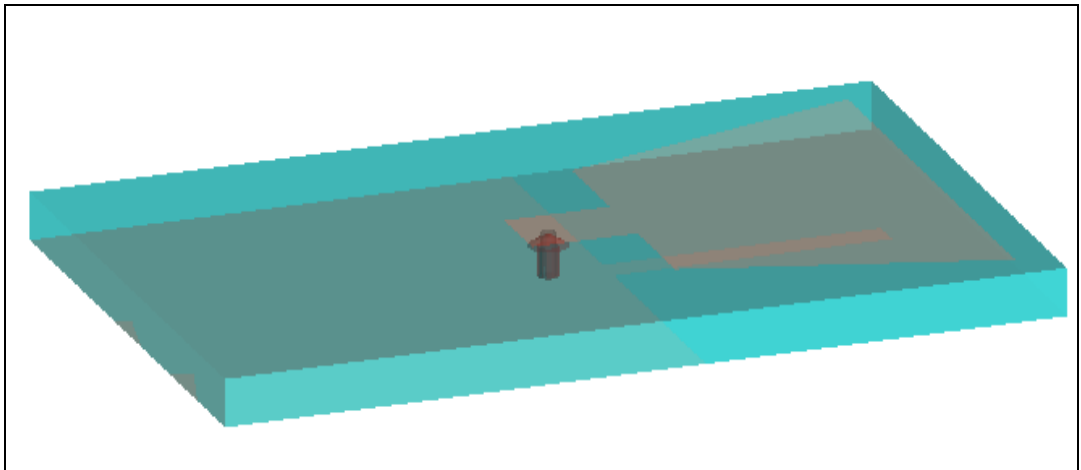


Figure 4.7. Transparent view of the UWB antenna with metamaterial contribution removed

4.1.3.1. VSWR Frequency bandwidth

In Figure 4.8. simulated VSWR frequency bandwidth of the two antennas, metamaterial based and conventional antennas are compared in order to determine effect of metamaterial properties contribution to the antenna performance. It is apparently seen from the Figure 4.8. that metamaterial antenna has larger VSWR frequency bandwidth. VSWR Frequency bandwidth of the metamaterial based antenna extends from 4GHz to 11.5GHz, where as frequency bandwidth of the conventional antenna extends from 4.2GHz to 7GHz.

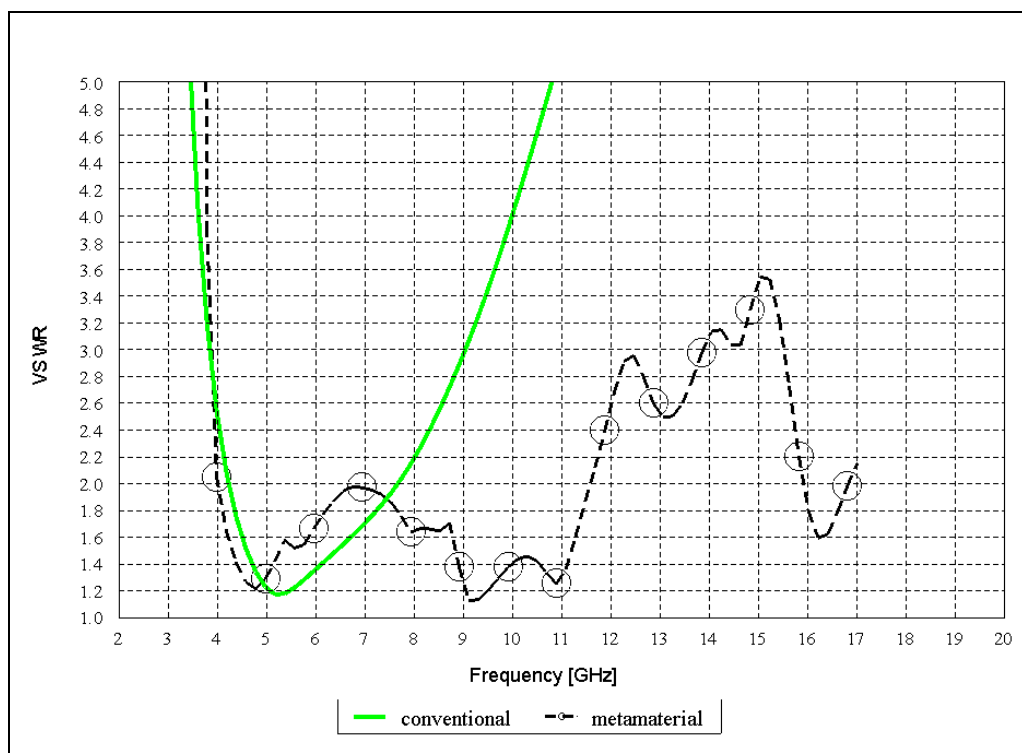


Figure 4.8. Comparison of VSWR bandwidth of the compact size UWB metamaterial antenna and same antenna with metamaterial contribution removed

It can be concluded that metamaterial based designs can have better input impedance matching over a wider frequency band.

4.1.3.2. Gain

In Figure 4.9. total gain of the antennas given in Figure 4.1. and Figure 4.6. is compared. It is apparently seen from the Figure 4.9. that conventional antenna has a higher gain at high

frequencies, compared to the UWB metamaterial antenna. On the other hand VSWR frequency bandwidth of the conventional antenna is very narrow as shown in Figure 4.8.

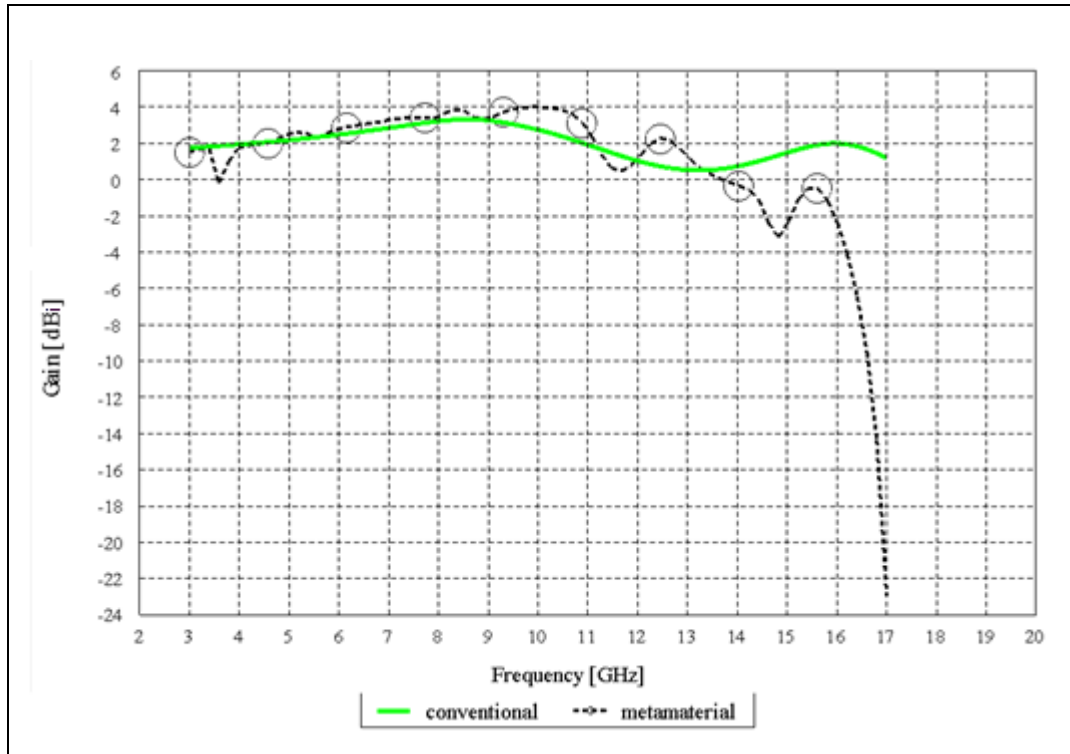


Figure 4.9. Comparison of total gain of the compact size UWB metamaterial antenna and same antenna with metamaterial contribution removed

4.2. COMPACT SIZE METAMATERIAL ANTENNA WITH RING SLOT

Rectangular ring slot is opened on the antenna as seen from the Figure 4.10. It is possible to see two rectangular ring slots on the antenna, the first one around the metallic cell which is connected to the ground potential by a via, the second rectangular ring slot is outside the parasitic metallic ring. The inner rectangular-slot is just a gap between metallic cell and surrounding metallic areas. The antenna is excited by a pin feed which is highlighted by a thick red arrow, and a short transmission line as shown in the Figure 4.10. and Figure 4.11. Antenna is designed using parameters of FR4 substrate with 1mm height.

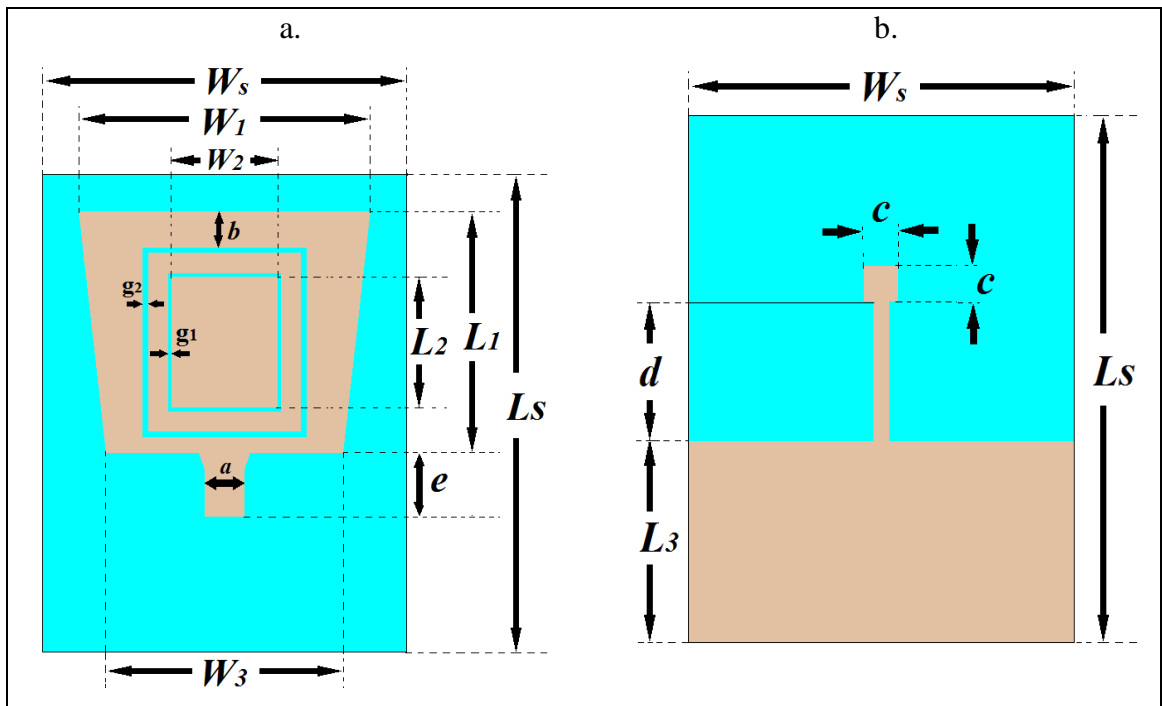


Figure 4.10. Compact size metamaterial antenna with ring slot a. Top view, b. Bottom view

Details of the dimensions for the antenna shown in Figure 4.10. are given table 4.1.

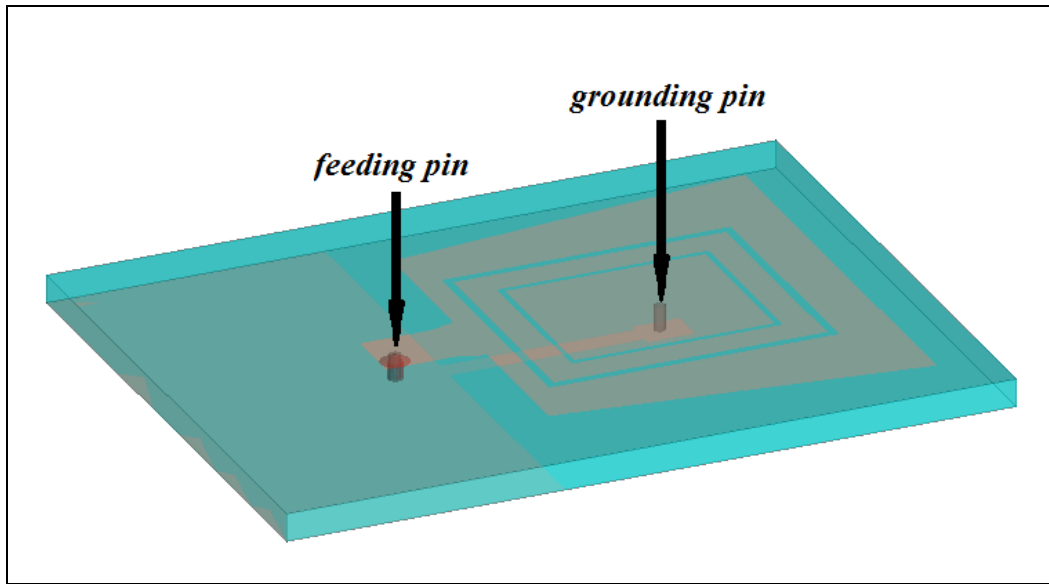


Figure 4.11. Transparent view of the compact size metamaterial antenna with ring slot

Table 4.1. Dimensions of metamaterial antenna with ring slot

Parameter	Magnitude (mm)	Parameter	Magnitude (mm)
t	0.8	d	7.7
b	2	s	1.5
g1	0.2	e	3.5
g2	0.3	c	1
Ws	18	Ls	26.2
W2	5.8	L1	13.3
W1	16	L2	7.2
W3	13	L3	10
a	2.2	thickness	1

Overall dimension of the antenna is 26.2mm x 18mm x 1mm. Total overall dimension of the ring slotted metamaterial antenna is larger than the design without ring slots.

4.2.1. VSWR Frequency Bandwidth

Frequency bandwidth of the antenna is shown in the Figure 4.12. Rectangular ring slots enhanced the matching of the antenna at low frequency bands compared with the design without ring slots, however addition of rectangular ring slots to the created notched bands within the frequency band. On the other hand inserting ring slot to antenna design improved the matching of the antenna between 14GHz and 16GHz.

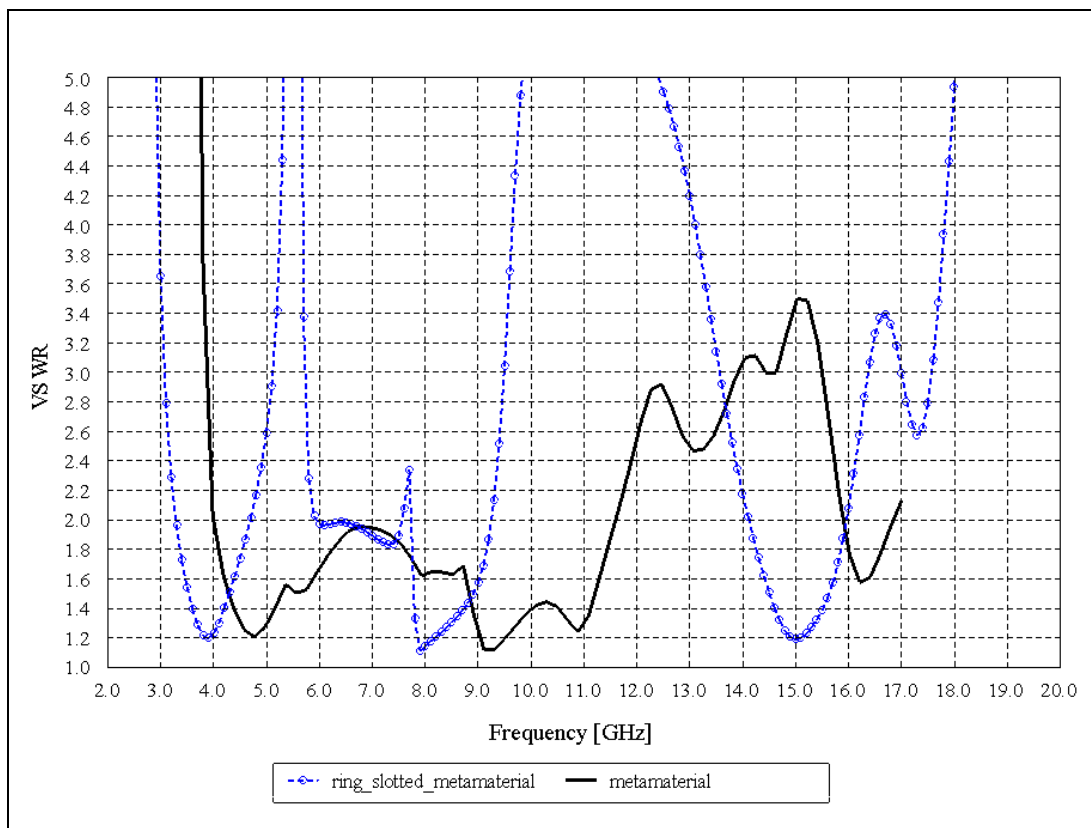


Figure 4.12. Simulated VSWR of compact size UWB metamaterial antenna with ring slot

4.2.2. Gain

Total gain of the antenna is given in Figure 4.13. Although the antenna has gain up to 14.3GHz, the gain of the antenna has many notched bands. Inserting ring slots to the antenna degraded the gain performance of the antenna.

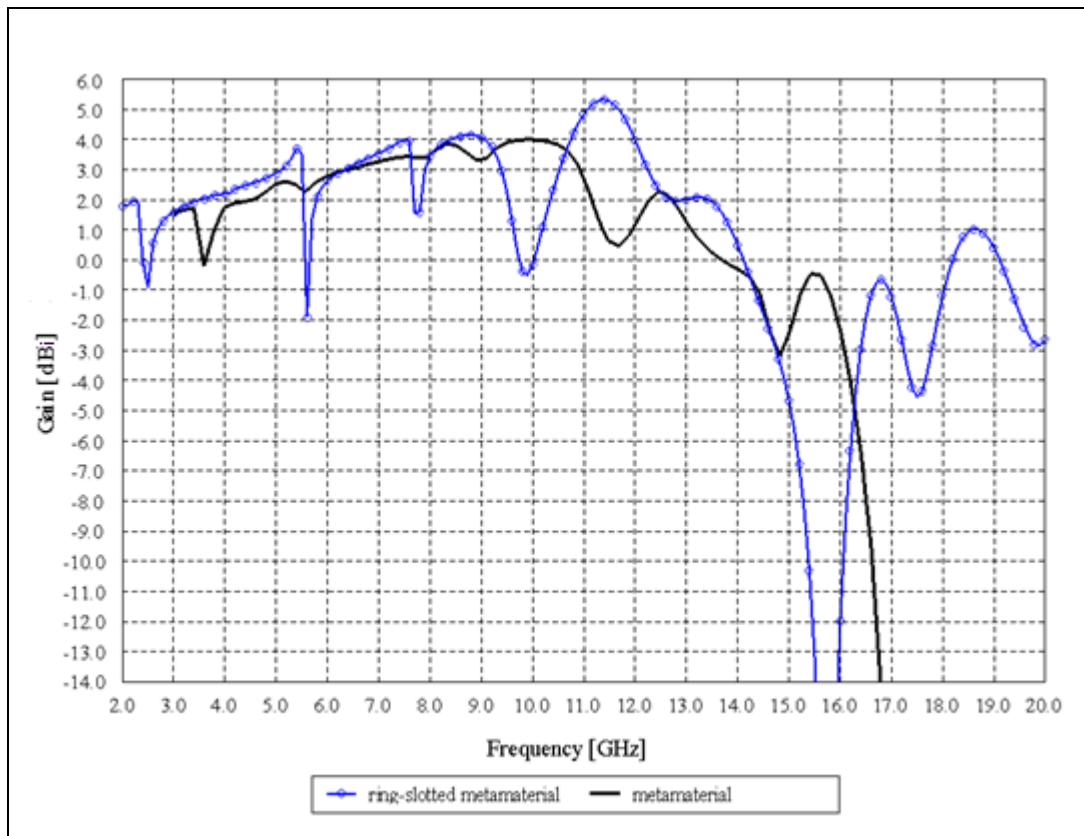


Figure 4.13. Total gain of compact size metamaterial antenna with ring-slot

4.3. COMPACT SIZE UWB METAMATERIAL ANTENNA WITH SPLIT RING SLOT

In Figure 4.14. and Figure 4.15. Detailed view of the designed compact size split-ring slotted metamaterial antenna is presented. Antenna is designed using the parameters of FR4 substrate with dielectric constant $4.3\epsilon_0$ and thickness 1mm. As shown in Figure 4.17. the metallic cell in the middle of the antenna is connected to the ground potential by a metal via and metallic cell on the antenna is capacitively coupled to the surrounding metallic structures as in the ring-slotted metamaterial antenna and tapered shape metamaterial antenna. Thus UWB split-ring antenna is CRLH metamaterial structure.

In the previous step the antenna which employs ring-slots have improved the matching of the antenna at low frequencies; however the design using ring slots created notched bands in the overall frequency band. Difference of this split-ring slotted metamaterial antenna from the ring slotted antenna design is outer rectangular-ring slot is replaced with

rectangular split-ring slot as depicted in Figure 4.15. In other words continuity of the outer rectangular- ring slot is cut by a metal while keeping the other dimensions same.

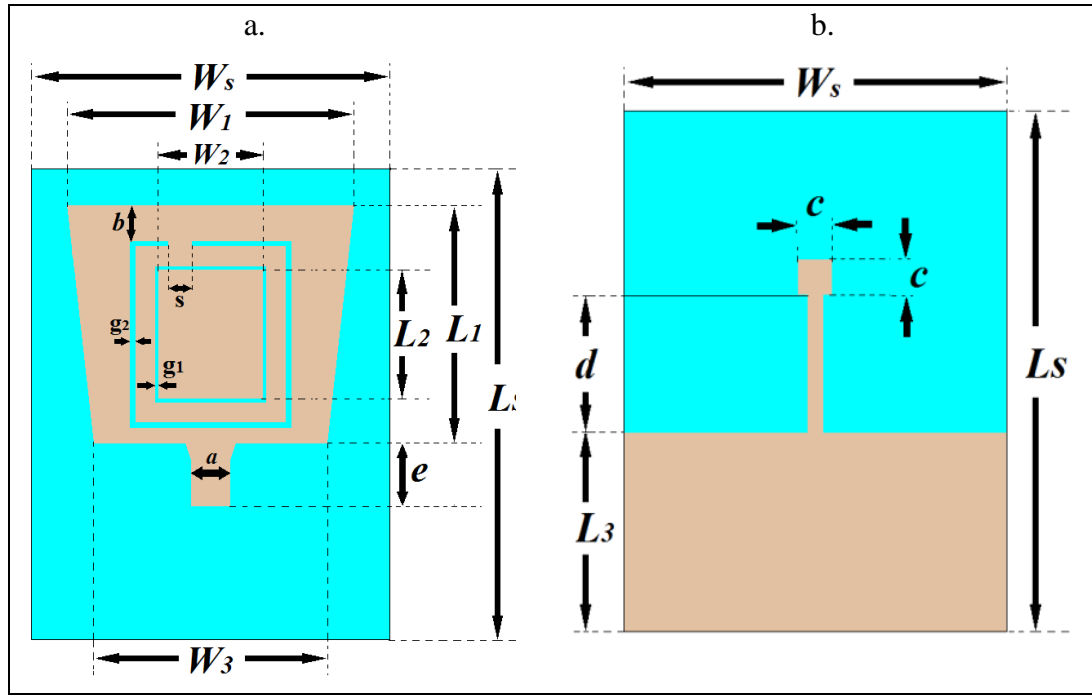


Figure 4.14. Compact size UWB metamaterial antenna with split-ring slot

a. Top view, b. Bottom view

Table: 4.2. Dimensions of compact size UWB metamaterial antenna with split-ring slots

Parameter	Magnitude (mm)	Parameter	Magnitude (mm)
W_s	18	L_s	26.2
W_1	16	L_1	13.3
W_2	5.8	L_2	7.2
W_3	13	L_3	10
a	2.2	c	1
b	2	d	7.7
g_1	0.2	e	3.5
g_2	0.3	s	1.5
t	0.8	thickness	1

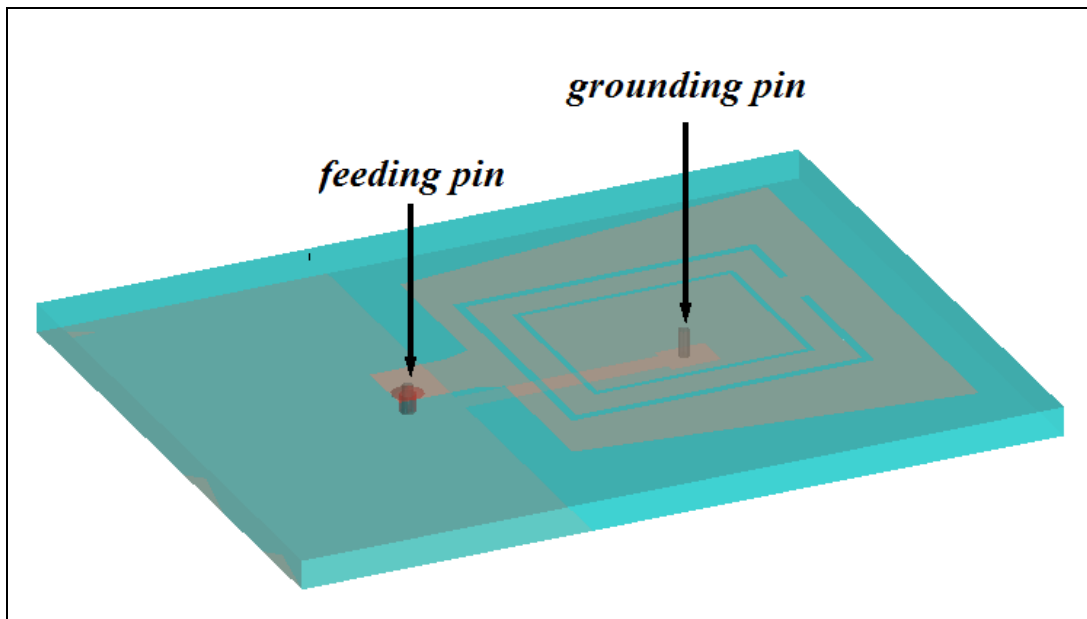


Figure 4.15. Transparent view of the compact size UWB metamaterial antenna split-ring slot

4.3.1. VSWR Frequency Bandwidth

Ring slot on the antenna is replaced with split-ring slot while keeping the other dimensions of the antenna same, as result the corresponding simulation VSWR result in Figure 4.16. is obtained. It is obviously seen from the Figure 4.17. using split-ring slot instead of ring slot eliminated spurious notched bands in the VSWR curve of the ring-slotted metamaterial antenna.

VSWR results of the designed antennas with ring slot and split ring slot, replacing ring slot with split ring slot eliminated spurious notched bands.

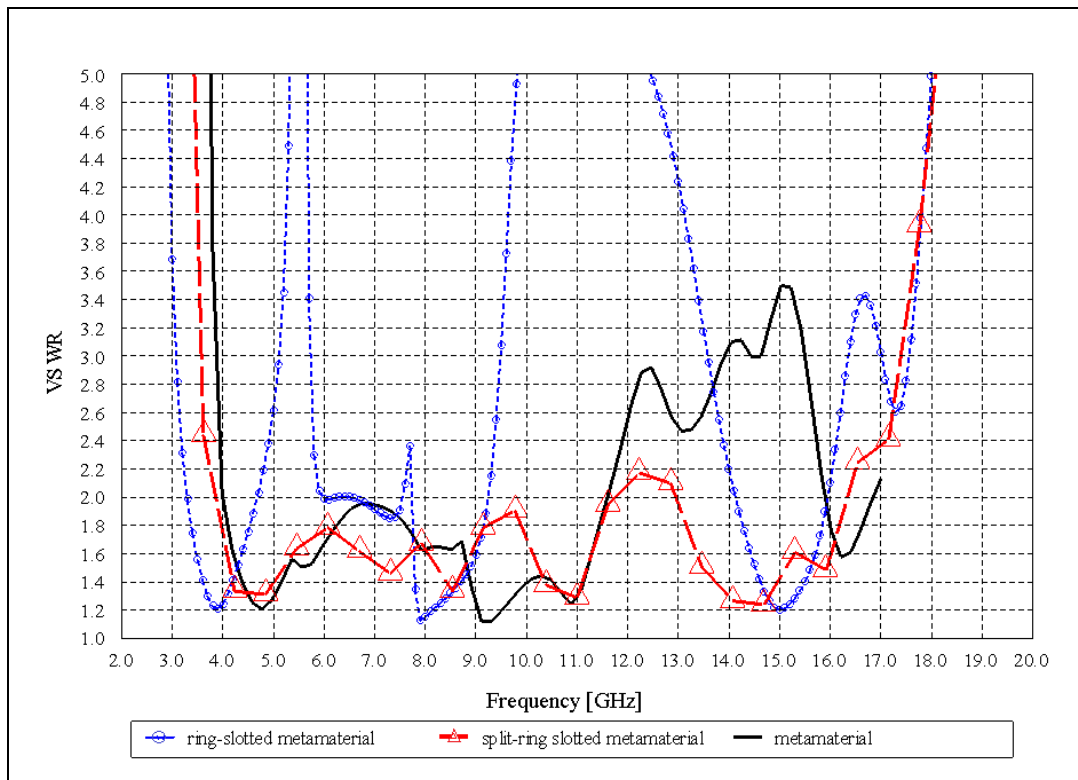


Figure 4.16. VSWR of compact size UWB metamaterial antennas

4.3.2. Gain

Total gain graphic of the UWB metamaterial antenna with ring slot is given in Figure 4.14. According to this figure antenna has gain larger than 0 dBi up to 15.5GHz.

Vertical and horizontal gain graphics of the antenna at different planes at three dimensional gain of the antenna at different frequencies are presented in polar graphics in the following Figures from 4.19. to Figure 4.21. According the radiation gain graphics antenna has omnidirectional radiation characteristics.

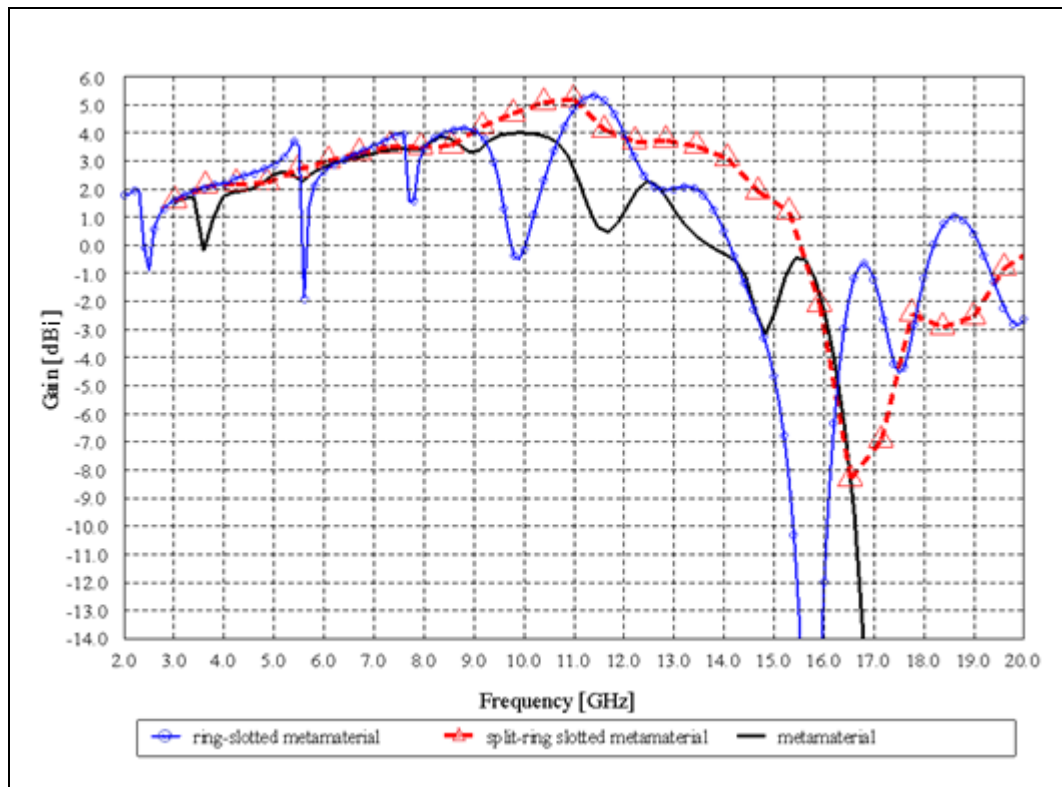


Figure 4.17. Total gain of compact size UWB metamaterial antennas

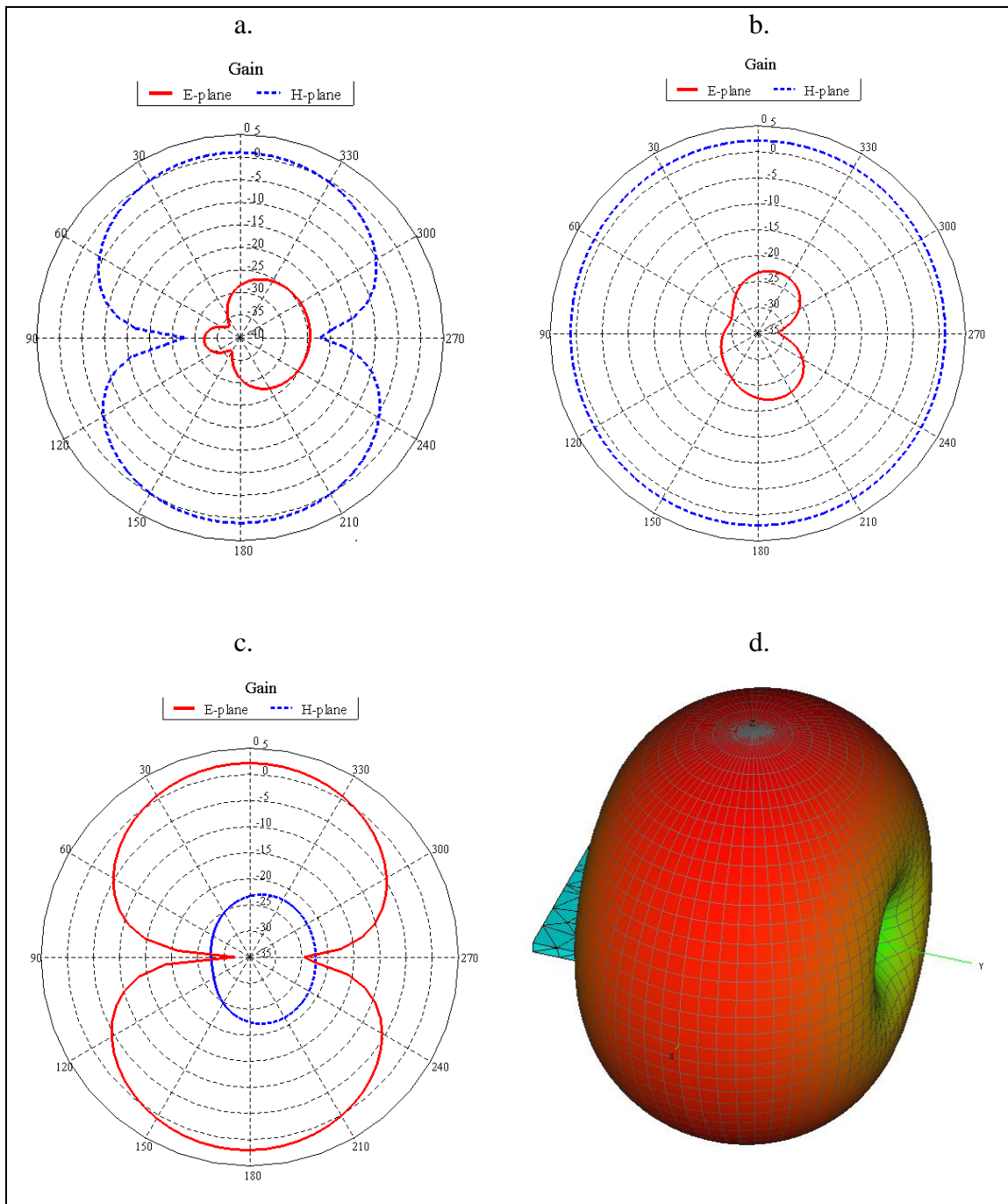


Figure 4.18. Simulated radiation patterns at 4.2 GHz a. x-y plane, b. x-z plane, c. y-z plane, d. 3D radiation plane

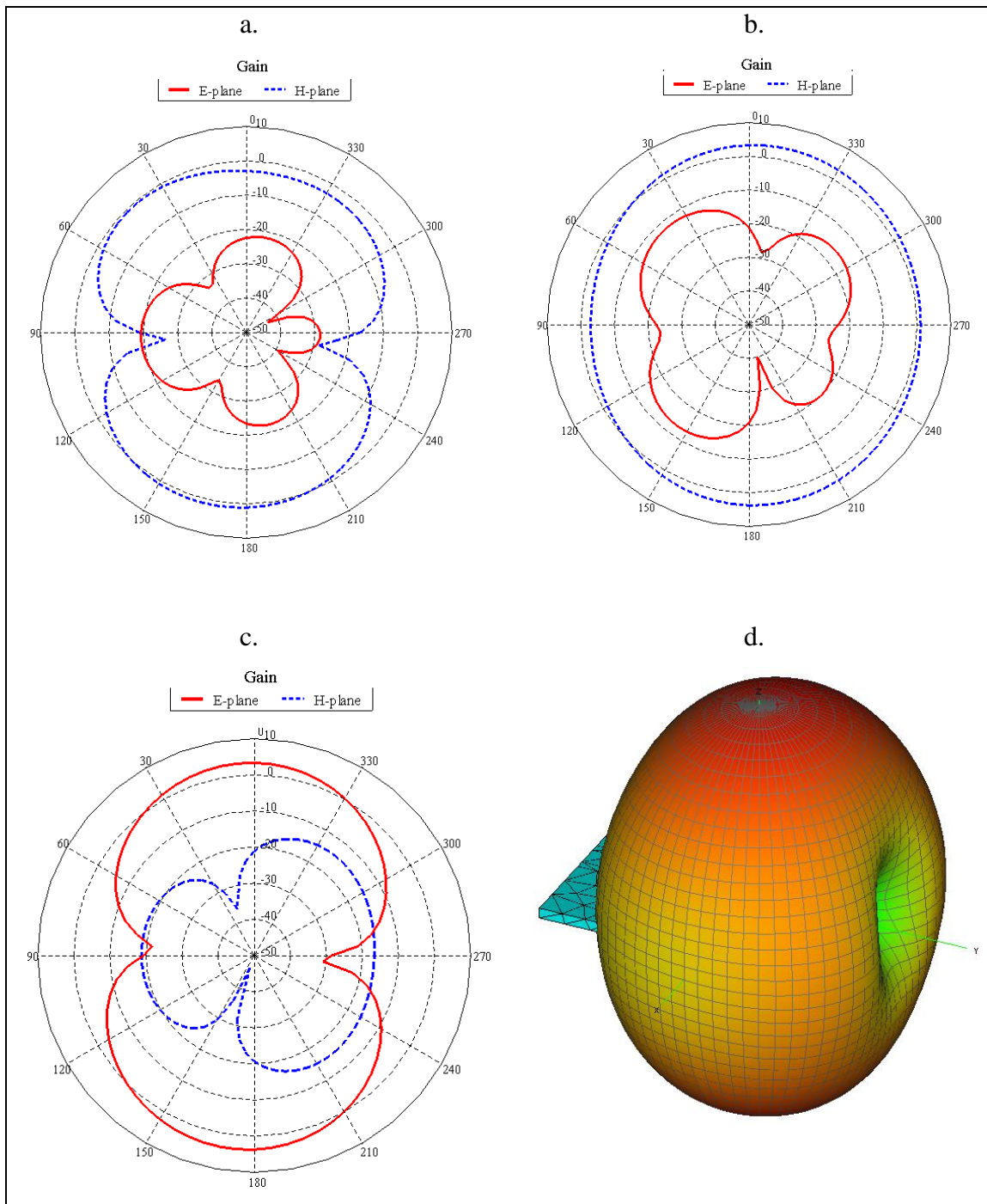


Figure 4.19. Simulated radiation patterns at 7.9 GHz a. x-y plane, b. x-z plane, c. y-z plane, d. 3D radiation pattern

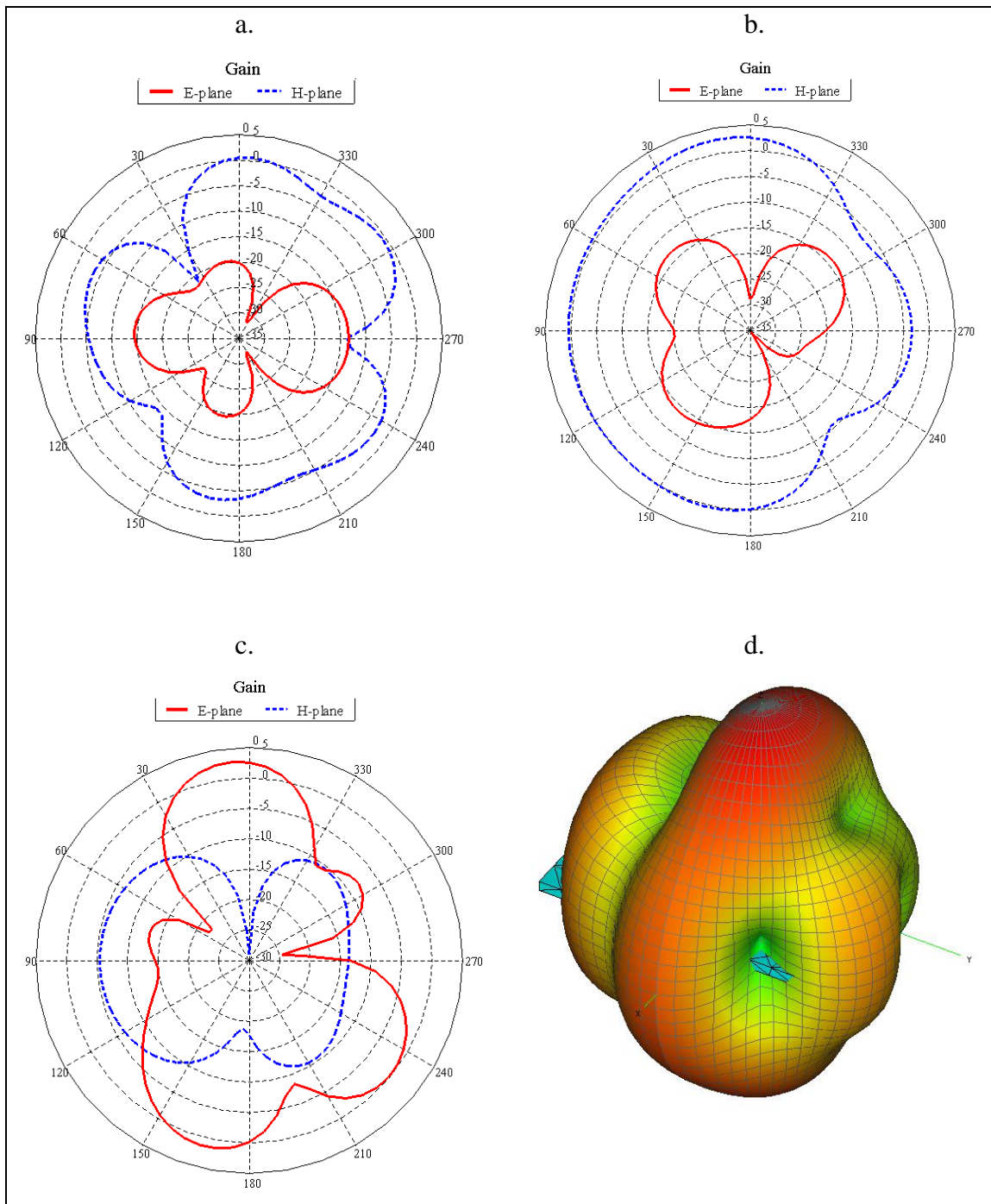


Figure 4.20. Simulated radiation patterns at 12.2 GHz a. x-y plane, b. x-z plane, c. y-z plane, d. 3D radiation pattern

5. COMPACT SIZE UWB METAMATERIAL ANTENNA REALIZATION and MEASUREMENTS

5.1. COMPACT SIZE UWB METAMATERIAL ANTENNA WITH RING SLOT

The designed compact size UWB ring-slotted metamaterial antenna presented in Figure 4.6. is fabricated on a FR4 substrate with height 1mm and dielectric constant $4.3\epsilon_0$. Antenna fabricated is shown in Figure 5.1. Dimensions of the antenna is same with the designed antenna and given in table 4.1.

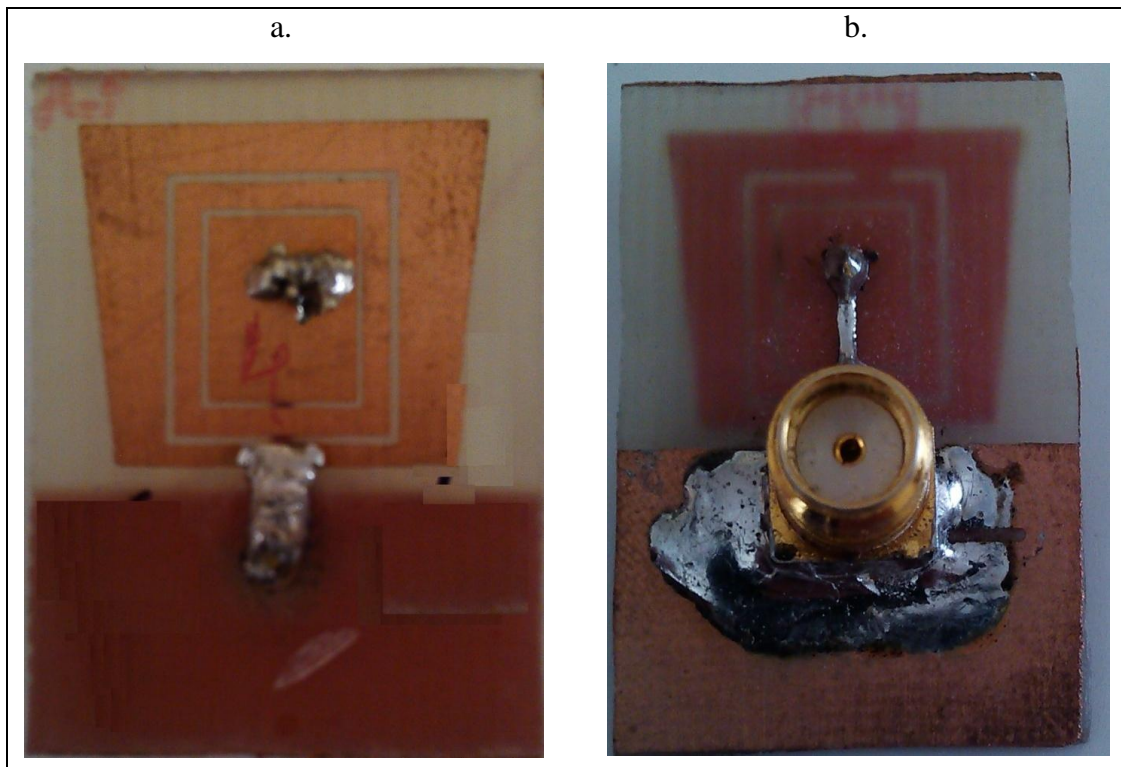


Figure 5.1. Compact size UWB metamaterial antenna with ring slots a. Top view,
b. Bottom view

VSWR measurement result of metamaterial antenna with ring slot is given in Figure 5.2.

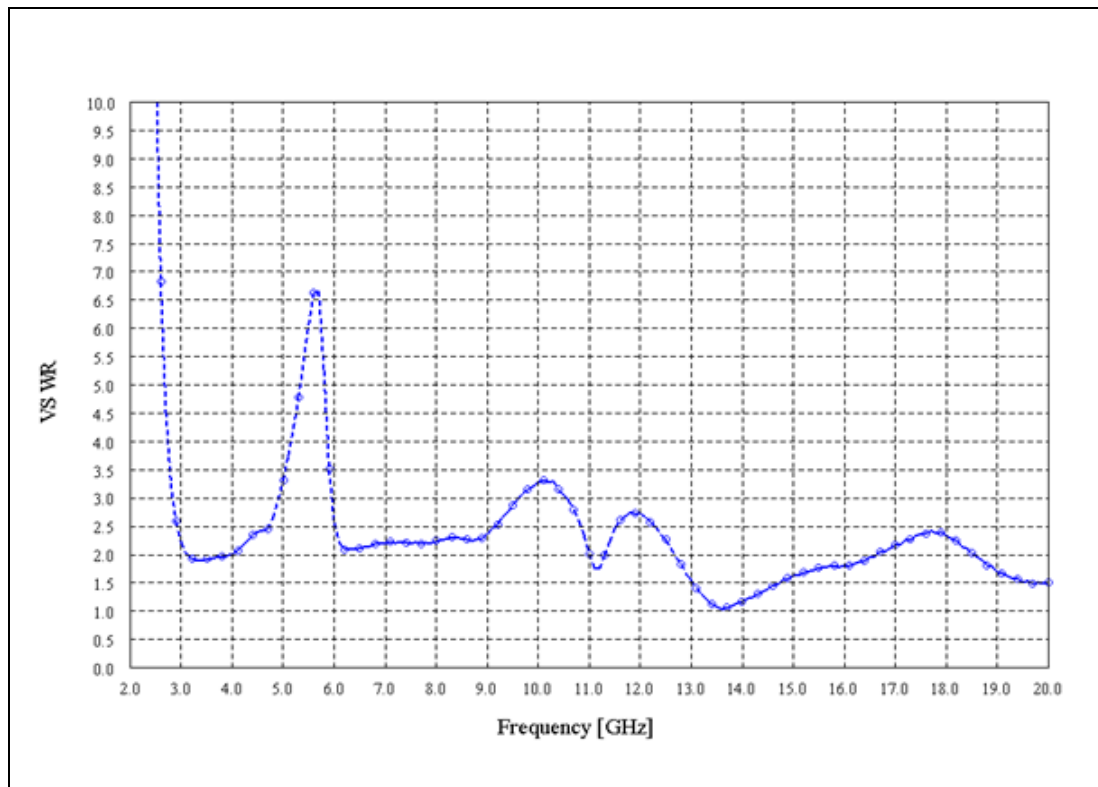


Figure 5.2. VSWR measurement result of compact size UWB metamaterial antenna with ring slot

Figure 5.3. shows the measured and simulated VSWR graphics of the ring-slotted compact size metamaterial antenna. Behavior of measurement and simulation VSWR graphics for the ring-slotted metamaterial antenna is roughly agreed with each other, especially at low frequencies.

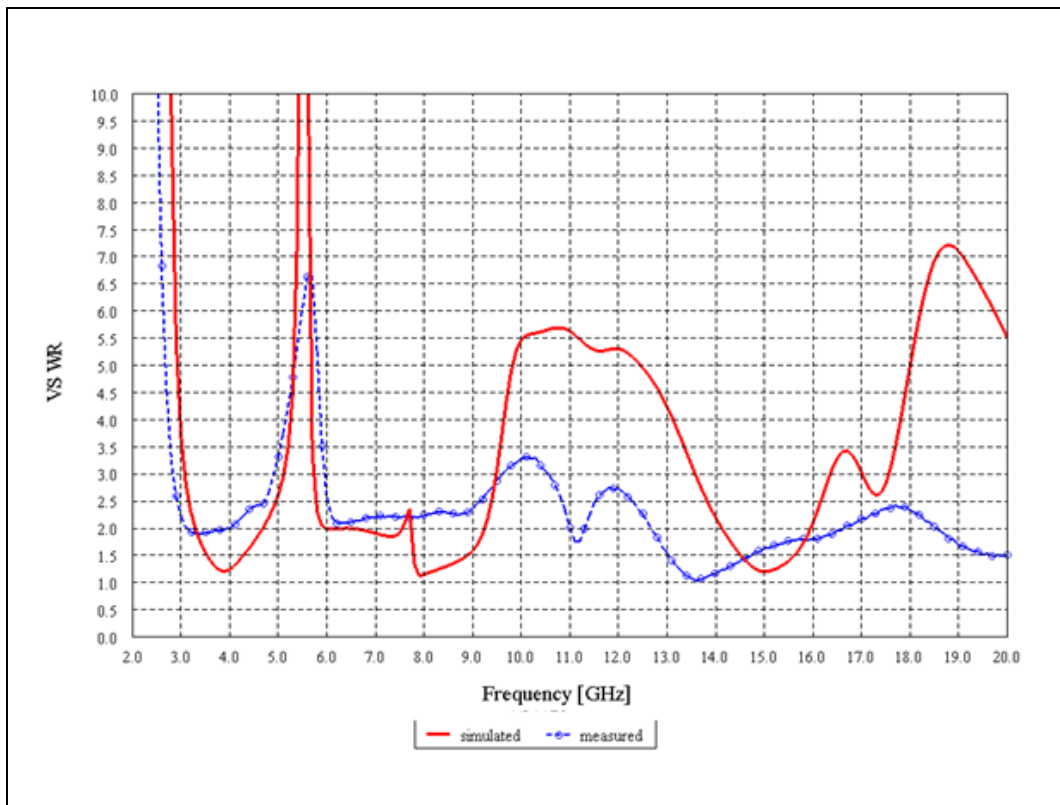


Figure 5.3. Comparison of measured and simulated results for compact size UWB metamaterial antenna with ring slot

5.2. COMPACT SIZE UWB METAMATERIAL ANTENNA WITH SPLIT RING SLOT

The designed split-ring-slotted compact size UWB metamaterial antenna presented in Figure 4.11. and Figure 4.12. is fabricated on a FR4 substrate with height 1mm and following Figure 5.4. shows the realized antenna. Dimensions of the antenna is same with the designed antenna and given in table 4.2.

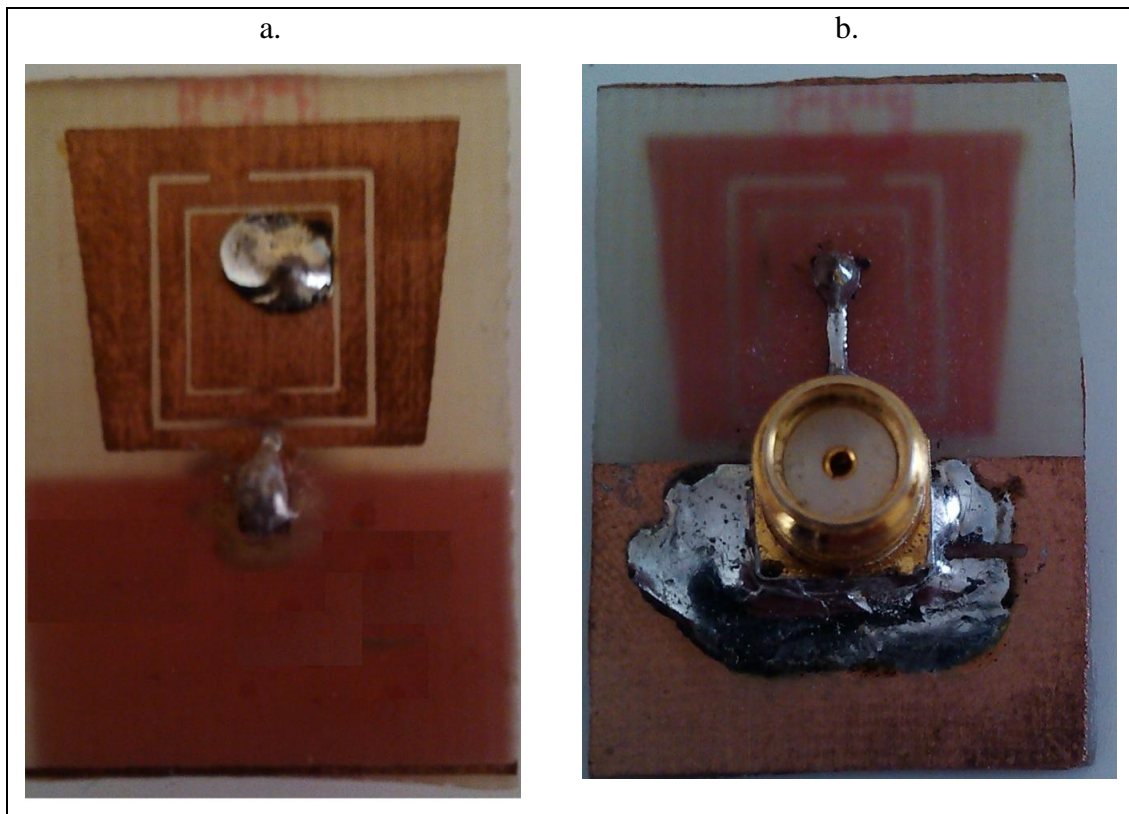


Figure 5.4. Compact size metamaterial antenna with split-ring slots a. Top view
b. Bottom view

In Figure 5.5. measurement result of the compact size UWB metamaterial antenna with split-ring slotted is given. As given in the graphic depicted in Figure 5.5. etching split-ring ring on the antenna improves VSWR bandwidth of the antenna. Metamaterial antenna with split ring slot has a better input impedance matching than the other antennas. VSWR value of the metamaterial antenna with split-ring slot is less than 2 from 4GHz to 7.88GHz and 8.28GHz to 17.55GHz, between 7.88GHz to 8.28GHz VSWR slightly larger than 2 but less than 2.2.

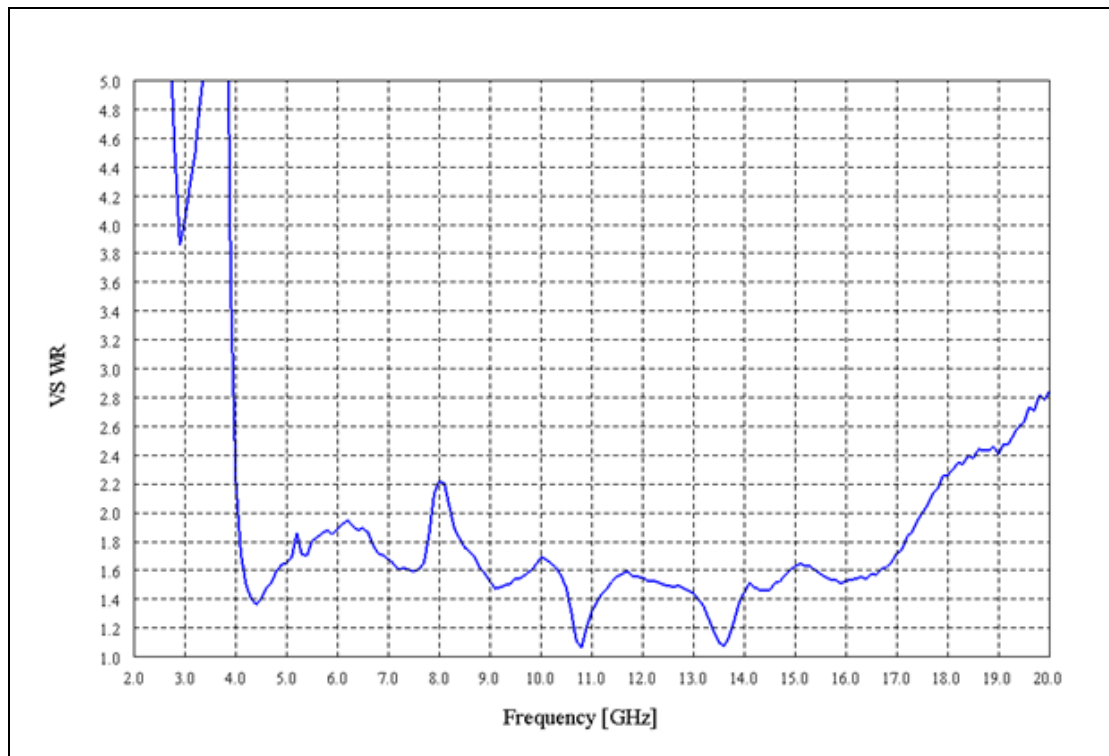


Figure 5.5. VSWR measurement result of compact size metamaterial antenna with split-ring slot

Simulated and measured VSWR graphics for compact size UWB metamaterial antenna with split-ring slot is given in Figure 5.6. It is apparently seen from Figure 5.6. that, simulation and measurement results are roughly agreed with each other. The minor discrepancies between the measured and simulated results may be caused by fabrication accuracy and deviation of dielectric constant from its designated value and handmade soldering.

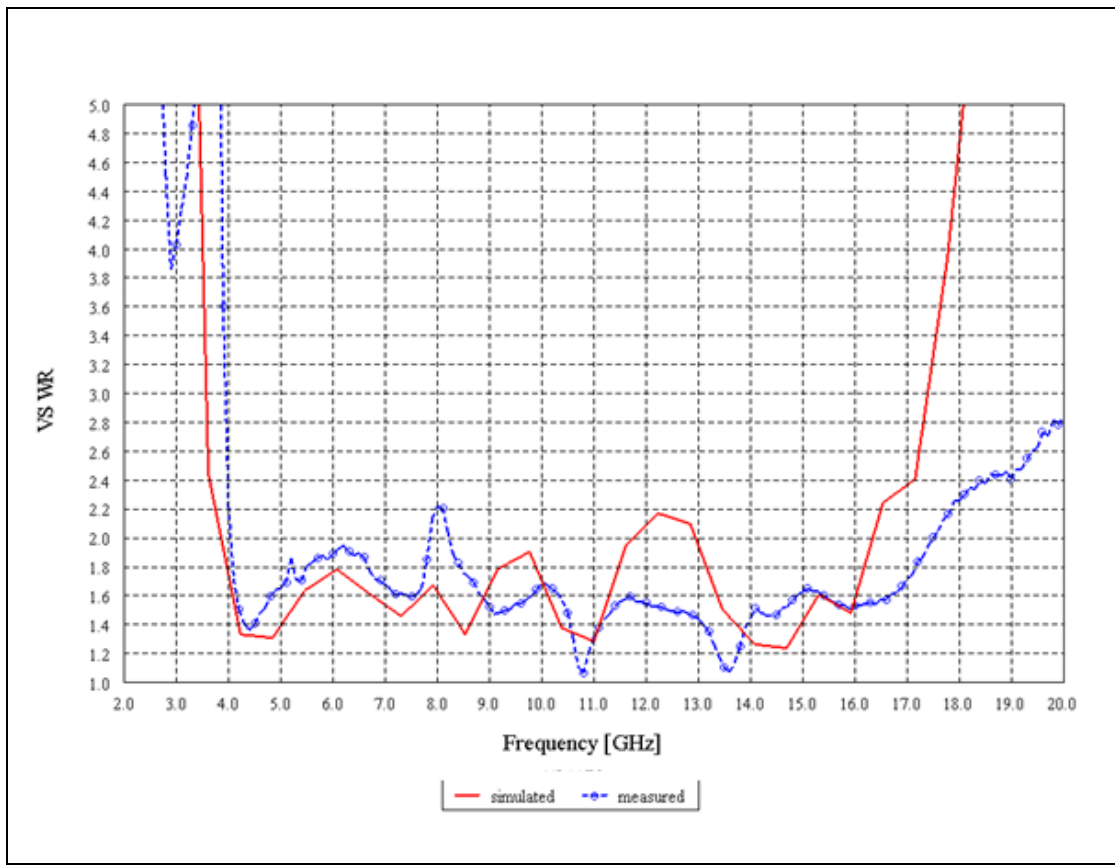


Figure 5.6. Comparison of measured and simulated results of compact size UWB metamaterial antenna with split-ring-slot

6. CONCLUSION

In this thesis compact size UWB metamaterial antennas are designed based on the concepts of CRLH transmission lines. In order to further enhance the frequency bandwidth of the antenna ring-slots are opened on the antenna however this ring slots created notched bands within the frequency bandwidth of the antenna and distorted the VSWR curve of the antenna. Thus ring slot on the antenna is replaced with split-ring slot which suppressed the VSWR value of the antenna in its frequency band eliminated notched bands and improved the matching of the antenna the.

Compact size ring slotted and split-ring slotted metamaterials antennas are manufactured on FR4 substrate with dielectric constant $4.3\epsilon_0$ and height of 1mm. Simulation and measurement results of the antennas are compared in Figures 5.3., and Figures 5.6. and it is seen that simulation and measurement results are mostly consistent with each other. It was proved that metamaterial can be used to design UWB antennas and they can improve the performance of the antenna.

Dimensions of the designed antennas are summarized in table 6.1. Inserting split-ring slots to the radiating patch improved the VSWR bandwidth of the antenna; however dimension of split-ring slotted antenna is larger than the initial designed antenna without slots

Table 6.1. Comparison of dimensions the designed antennas

	Material	Dielectric constant	Width	Length	Height
Metamaterial Antenna	FR4	$4.3\epsilon_0$	14mm	21mm	1mm
Metamaterial Antenna with ring slots	FR4	$4.3\epsilon_0$	18mm	26.2mm	1mm
Metamaterial Antenna with split-ring slot	FR4	$4.3\epsilon_0$	18mm	26.2mm	1mm

Figure 6.1. shows the VSWR curve of the designed antennas. Inserting ring slots on the compact size UWB metamaterial antenna improved the VSWR of the antenna at low frequencies, lower than 4GHz, and frequency between 14GHz and 16GHz; however; it

created spurious resonance within the frequency band of the antenna. In order to get rid of these undesired resonances, split-ring slot is used instead of ring slot. As expected VSWR frequency bandwidth of the antenna is improved. It is obviously seen that that design with split-ring slot have much larger frequency bandwidth with $VSWR < 2$.

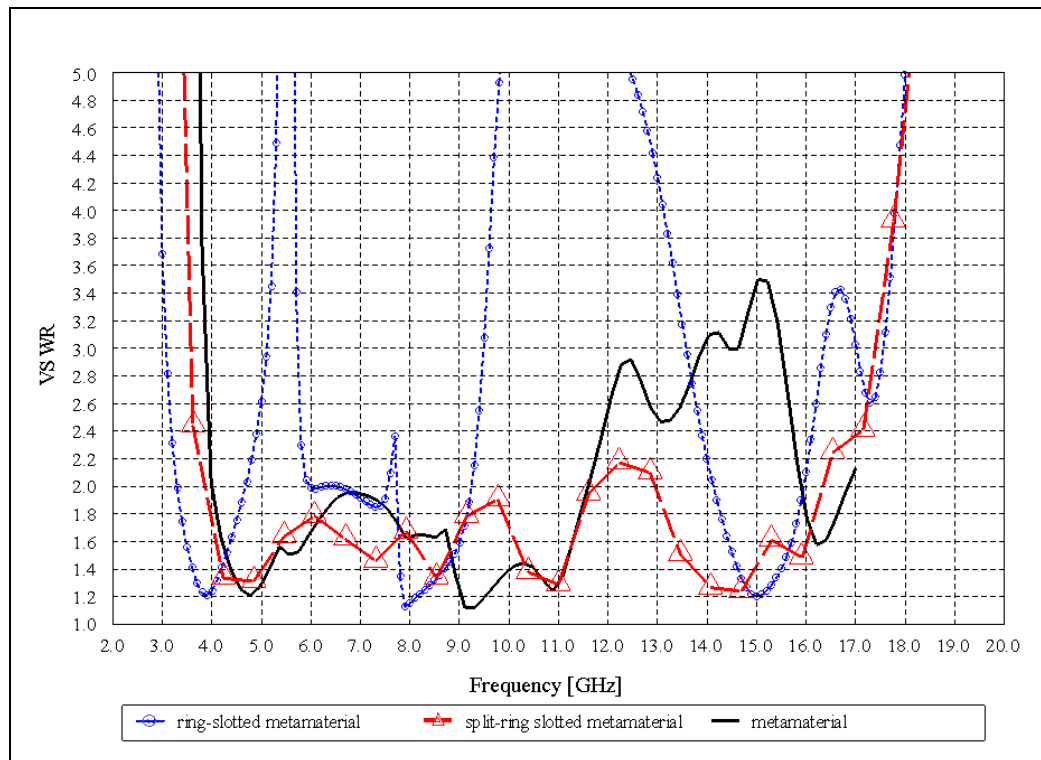


Figure 6.1. Comparison of simulated VSWR results for all designed antennas

In figure 6.2 simulated total gain graphic of all designed antennas are shown. It is obviously seen that compact size UWB metamaterial antenna with split ring slot have better gain performance.

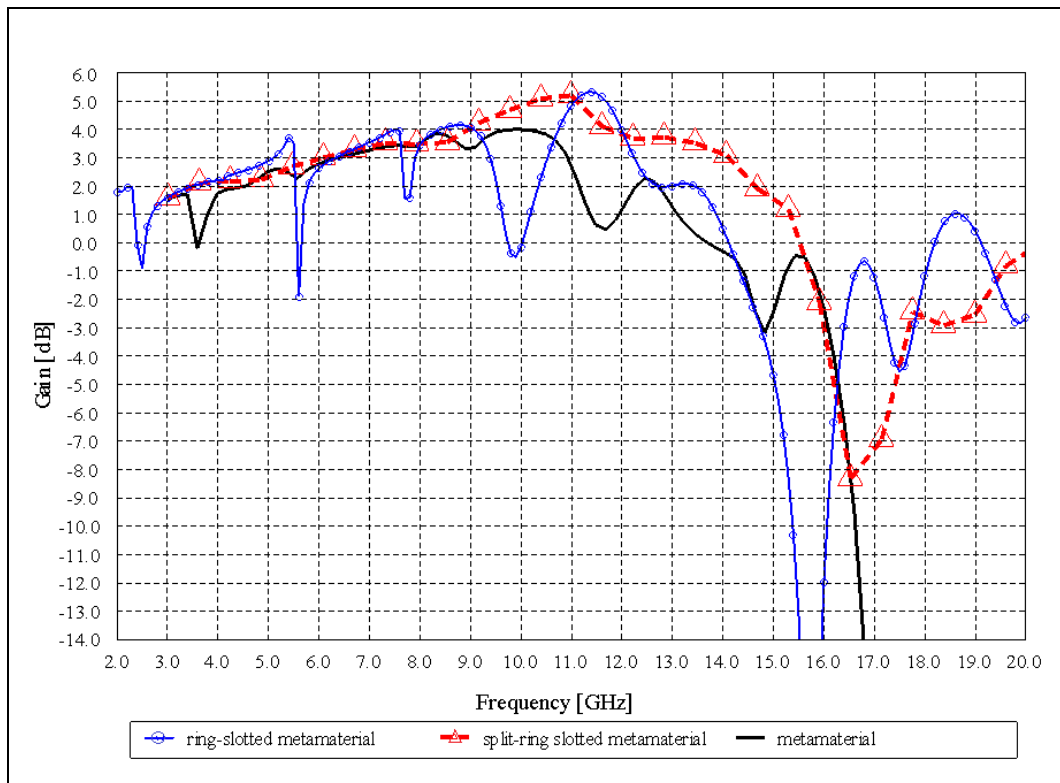


Figure 6.2. Comparison of total gain of all designed antennas

In Figure 6.3. measured VSWR results of the compact size UWB metamaterial antenna with ring slot and compact size UWB metamaterial antenna with split-ring slot are shown. According to that figure, comparison of the VSWR measurement results of metamaterial antenna with ring slot and metamaterial antenna with split ring slot verify the simulated outcomes that using split-ring slots instead of ring slots improves VSWR frequency bandwidth of the antenna.

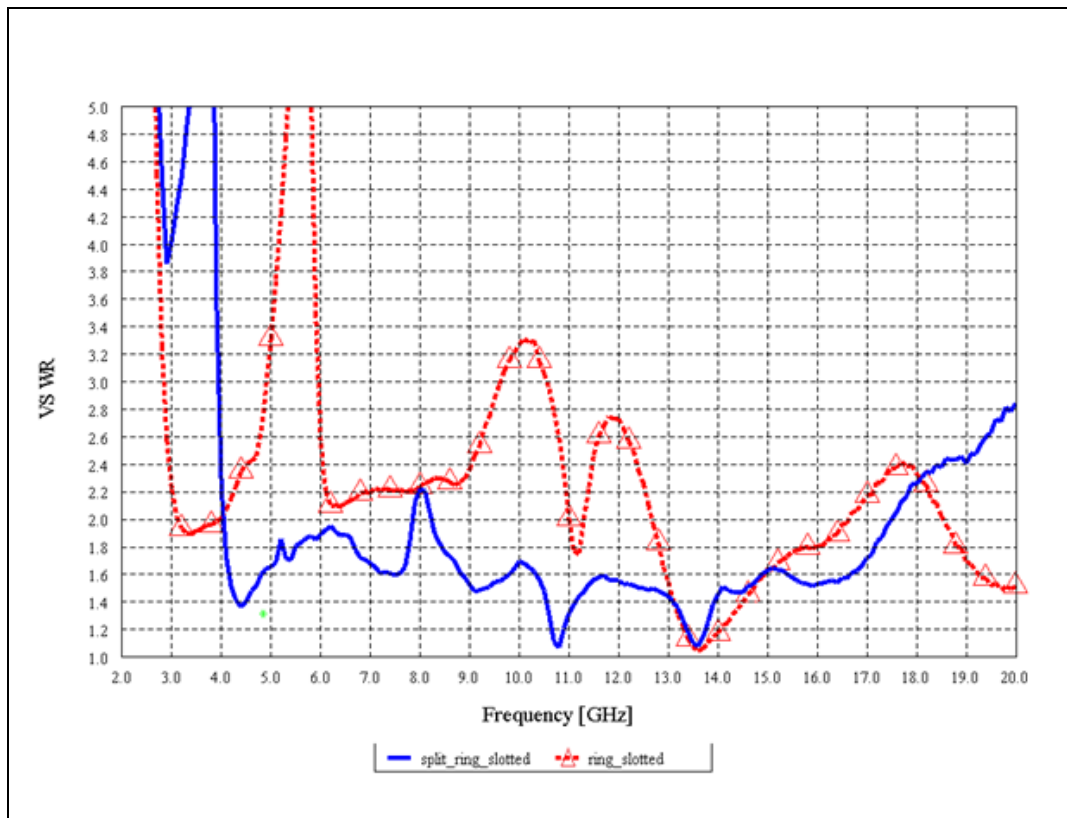


Figure 6.3. Comparison of measured VSWR results for compact size UWB metamaterial antenna ring-slot and split-ring-slot

Table 6.3. Summary of the performance for compact size UWB metamaterial antenna with split-ring slots

	simulated	measured
VSWR < 2	3.8GHz--16.4GHz	4GHz—17.5GHz
Total Gain > 0 dBi	Up to 15.5GHz	Not available

Although designed and manufactured compact size UWB metamaterial antenna has dimension of 26.2mm x 18mm, antenna can successfully cover a large frequency band as shown in table 6.3. Measurement results did not exactly match the simulation results. Measurements were not made in an anechoic chamber, and behavior of FR4 material in high frequencies is not exactly given in datasheets. Furthermore manufacturing and handmade work tolerances.

In conclusion compact size UWB metamaterial antenna with split-ring slot can be successfully used in compact size high data rate wireless application like wireless dongle USB applications, body wear health monitoring applications. As future work dispersion of the designed antenna can be analyzed.

REFERENCES

1. K. L. Wong, *Planar Antennas for Wireless Communications*, Wiley-Interscience, 2003.
2. James Baker, Dejan Filipović, "Ultra-Wideband antennas", *International Journal of Antennas and Propagation*, Hindawi Publishing Corporation, Vol., 2008.
3. Samaddar, S.N.; Mokole, E.L., "Biconical antennas with unequal cone angles", *Antennas and Propagation, IEEE Transactions on*, Vol.46, pp.181-193, Feb 1998.
4. J. R. James and P. S. Hall, *Handbook of Microstrip antennas*. London: IEE – Peter Peregrinus, Ltd. (IEE Electromagnetic Waves Series. Volume 28), 1989.
5. Qi; Xu Shan-jia, "Composite right/left handed transmission line metamaterials and applications", *Metamaterials, 2008 International Workshop on*, Vol., pp.72-75, 9-12 Nov. 2008.
6. Stutzman, *Antenna Theory and Design*, 2nd ed., Wiley, New York, 1998.
7. Liu Qing., *Antennas Using Left Handed Transmission Lines, Phd. Report*, PhD Report, University of Birmingham, 2009.
8. Wei Huang; Nan Xu; Pathak, V.; Poilasne, G.; Achour, M.; , "Composite Right-Left Handed Metamaterial ultra-wideband antenna", *Antenna Technology*, 2009. iWAT 2009. IEEE International Workshop on , Vol., pp.1-4, 2-4 March 2009.
9. Bimal Garg, Mayank Gautam., "Microstrip Patch Antenna using Left-Handed Metamaterial Structure for Bandwidth Improvement", *International Journal of Electronics & Communication Technology*, Vol.2 Issue 3, Sept. 2011.

10. Brennan, E.; Fusco, V.; Schuchinsky, A., "Investigation on properties of left-handed materials", *High Frequency Postgraduate Student Colloquium*, 2003, Vol., pp. 65- 68, 8-9 Sept. 2003.
11. Bo Zhao; Ruirong Shi; Ferendeci, A.M., "Zeroth-Order Resonator Antennas Using Composite Right/Left-Handed Microstrip Transmission Lines", *Aerospace and Electronics Conference*, 2008. NAECON 2008. IEEE National , Vol., pp.154-158, 16-18 July 2008.
12. Seung-Tae Ko; Jeong-Hae Lee, "Broadband metamaterial antenna using folded parasitic patch", *Antennas and Propagation (APSURSI), 2011 IEEE International Symposium on*, Vol., pp.1051-1053, 3-8 July 2011.
13. J. H. Park, Y. H. Ryu, and J. H. Lee "Mu-zero Resonance Antenna", *IEEE Transaction on Antennas and Propagation*, Vol. 58, pp. 1865-1875, June 2010.
14. Mishra, D.; Arun Kumar, G.; Poddar, D.R.; Mishra, R.K., "Simulated resonant characteristics of embedded metamaterial patch antenna", *Applied Electromagnetics Conference*, 2007. AEMC 2007. IEEE , Vol., pp.1-3, 19-20 Dec. 2007.
15. Ben Issa, I.; Rian, R.; Essaaidi, M., "Circularly polarized microstrip patch antenna gain improvement using new left-handed metamaterial structure", *Microwave Symposium (MMS), 2009 Mediterranean* , Vol., pp. 1-3, 15-17 Nov. 2009.
16. Garg, B.; Sabharwal, A.; Shukla, G.; Gautam, M., "Microstrip Patch Antenna Incorporated with Left Handed Metamaterial at 2.4 GHz", *Communication Systems and Network Technologies (CSNT), 2011 International Conference on*, Vol., pp.208-210, 3-5 June 2011.
17. Andrea Alù, "Subwavelength, compact, resonant patch antennas loaded with metamaterials", *IEEE Transaction on Antennas and Propagation*, Vol. 55, 2007.
18. Matthew Mishrikey, *Analysis and Design of Metamaterials*, PhD Report,

Massachusetts Institute of Technology, Cambridge MA, USA.

19. C.Caloz and T. Itoh, *Electromagnetic Metamaterials: Transmission Line Theory and Microwave Applications*, New York, Wiley, 2004.
20. Constantine A. Balanis. *Antenna theory, analysis and design*, John Wiley & Sons, 3rd.edition, 2005.
21. R. Marques, F. Martin, M. Sorolla, *Metamaterials with negative parameters*, John Wiley and Sons, New York, 2008.
22. Yan Zhang; Wei Hong; Chen Yu; Zhen-Qi Kuai; Yu-Dan Don; Jian-Yi Zhou, "Planar Ultrawideband Antennas With Multiple Notched Bands Based on Etched Slots on the Patch and/or Split Ring Resonators on the Feed Line", *Antennas and Propagation, IEEE Transactions on*, Vol.56, pp.3063-3068, Sept. 2008.
23. Hsueh-Chuan Tang; Ken-Huang Lin;, "Design of A UWB antenna for wireless USB dongle application", *Microwave Conference*, 2009. APMC 2009. Asia Pacific, Vol., pp.786-789, 7-10 Dec. 2009.
24. Salmani, Z.; Hualiang Zhang;, "Log-periodic antenna array inspired parallel strip ultra-wideband (UWB) antenna", *Radio and Wireless Symposium (RWS)*, 2011 IEEE, Vol., pp.283-286, 16-19 Jan. 2011.
25. Longjun Zhang; Fushun Zhang; Zhenlin Liao; Pu Wan; Gaoli Ning; , "A miniaturized, omni-directional UWB biconical antenna with band-notched", *Microwave, Antenna, Propagation, and EMC Technologies for Wireless Communications (MAPE)*, 2011 *IEEE 4th International Symposium on* , Vol., pp.116-119, 1-3 Nov. 2011.
26. Kudpik, R.; Siripon, N.; Meksamoot, K.; Kosulvit, S., "Design of a compact biconical antenna for UWB applications", *Intelligent Signal Processing and Communications Systems (ISPACS)*, 2011 *International Symposium on*, Vol., pp.1-6,d 7-9 Dec. 2011.

27. Khemphila, Anchana; Promwong, Sathaporn;, "Ultra Wideband Network in Short-Range Wireless System for Personal Computer", *Communications and Information Technologies, 2006. ISCIT '06. International Symposium on*, Vol., pp.1221-1224, Oct. 18 2006-Sept. 20 2006.
28. Calmon, A.; Pacheco, G.; Terada, M.;; "A novel reconfigurable UWB log-periodic antenna", *Antennas and Propagation Society International Symposium 2006, IEEE* , Vol., pp.213-216, 9-14 July 2006.
29. Qi Wu; Ronghong Jin; Junping Geng;, "A Single-Layer Ultrawideband Microstrip Antenna", *Antennas and Propagation, IEEE Transactions on* , Vol.58, pp.211-214, Jan. 2010.
30. Nashaat, D.; Elsadek, H.A.; Abdallah, E.; Elhenawy, H.; Iskander, M.F.;"Enhancement of ultra-wide bandwidth of microstrip monopole antenna by using metamaterial structures", *Antennas and Propagation Society International Symposium, 2009. APSURSI '09. IEEE* , Vol., pp.1-4, 1-5 June 2009.
31. Pires, N., Letizia, M.; Maisenbacher, A., "Design of an Ultra Wideband Universal Serial Bus device mounted antenna", *Antenna Technology (iWAT), 2010 International Workshop on* , Vol., pp.1-4, 1-3 March 2010.
32. Adesoji Sajuyigbe., *Electromagnetic Metamaterials for Antenna Applications*, PhD Report, Duke University, 2010.
33. Sihvola, A., "Metamaterials in electromagnetics", *Metamaterials*, Vol. 1, pp. 2-11, 2007.
34. Samantha Caporal Del Barrio., *Enhancement of Electrically Small Antennas Properties with Metamaterials*, M.S. Report, AALBORG University,Denmark, 2010
35. R. Ludwig and P. Bretchko, *RF Circuit Design: Theory and Applications*, Pearson Education Inc. Prentice Hall, 2000.

36. Eleftheriades, G.V.; Iyer, A.K.; Kremer, P.C.;, "Planar negative refractive index media using periodically L-C loaded transmission lines", *Microwave Theory and Techniques, IEEE Transactions on*, Vol. 50, pp. 2702- 2712, Dec. 2002
37. COLLIN, R. E., *Field Theory of Guided Waves*, IEEE Press, Piscataway, N. J., 1991,
38. Xin Hu., *Some Studies on metamaterial transmission lines and their applications*, PhD Report Stockholm, Sweden, 2009.
39. Hunda Bin A. Majid., *Left Handed Metamaterial Incorporated with Microstrip Antenna*, M.S. Report, Universiti Teknologi Malaysia, 2010.
40. Wiesbeck, W.; Adamiuk, G.; Sturm, C.; , "Basic Properties and Design Principles of UWB Antennas", *Proceedings of the IEEE* , Vol. 97, pp.372-385, 2009
41. Schantz, H.G., "A brief history of UWB antennas", *Ultra Wideband Systems and Technologies*, 2003 IEEE Conference on , Vol. 2, pp. 209- 213, 16-19 Nov. 2003
42. V. G. Veselago, "The electrodynamics of substances with simultaneously negative values of ϵ and μ " *Soviet Phys. Uspekhi*, Vol. 10, pp. 509–514, 1968.